Matching coefficients for α_s and m_b to $\mathcal{O}(\alpha_s^2)$ in the MSSM

JHEP02(2009)037

(http://iopscience.iop.org/1126-6708/2009/02/037)

Published by IOP Publishing for SISSA
Received: *October 29, 2008*
Revised: *January 12, 2009*
Accepted: *January 16, 2009*
Published: *February 12, 2009*

JHEP02(2009)037

Matching coefficients for α_s and m_b to $\mathcal{O}(\alpha_s^2)$ in the MSSM

A. Bauer, L. Mihaila and J. Salomon

Institut für Theoretische Teilchenphysik, Universität Karlsruhe (TH),
Karlsruhe Institute of Technology (KIT),
76128 Karlsruhe, Germany
E-mail: andreas.bauer@zsw-bw.de, luminita@particle.uni-karlsruhe.de, salomon@particle.uni-karlsruhe.de

Abstract: We compute the exact two-loop matching coefficients for the strong coupling constant α_s and the bottom-quark mass m_b within the Minimal Supersymmetric Standard Model (MSSM), taking into account $\mathcal{O}(\alpha_s^2)$ contributions from Supersymmetric Quantum Chromodynamics (SQCD). We find that the explicit mass pattern of the supersymmetric particles has a significant impact on the predictions of α_s and m_b at high energies. Further on, the three-loop corrections exceed the uncertainty due to the current experimental accuracy. In case of the the running bottom-quark mass, they can reach in the large $\tan\beta$ regime up to 30% of the tree-level value.

Keywords: Supersymmetry Phenomenology.

Contents

JHEP02(2009)037

1. Introduction

Supersymmetry (SUSY) is currently believed to play an important role in physics beyond the Standard Model (SM). A compelling argument in favour of SUSY is the particle content of the MSSM, that leads in a natural way to the unification of the three gauge couplings at a high energy scale $\mu \simeq 10^{16}\,\text{GeV}$, in agreement with predictions of Grand Unification Theories (GUT) [1 – 3].

Apart from the gauge coupling unification, in GUT models based on simple groups such as SU(5) [4] or SO(10) [5], also the bottom (y_b) and tau (y_τ) Yukawa couplings unify at the GUT scale. For some models based on SO(10) (or larger groups) even the unification of the bottom, tau and top (y_t) Yukawa couplings is predicted. However, the condition of Yukawa coupling unification can be fulfilled within the MSSM only for two regions of $\tan\beta$, the ratio of Higgs field vacuum expectation values: $\tan\beta \approx 1$ and $\tan\beta \approx 50$ [6 – 8]. A main feature of SUSY models with large $\tan\beta$ is that the supersymmetric radiative corrections to fermion masses and couplings can be as large as the leading order (LO) contributions [7, 9, 10]. This renders the knowledge of the higher order (HO) corrections in perturbation theory mandatory. On the other hand, the unification condition becomes very sensitive to the low energy parameters [11]. This property can be exploited to greatly constrain the allowed MSSM parameter space.

With the advent of the CERN Large Hadron Collider (LHC), we will be able to probe the realization of SUSY in nature to energy scales of $\mathcal{O}(1)\,\text{TeV}$. In particular, precision

measurements and computations will allow to test the low-energy supersymmetric relations between the particle masses and couplings. It is often argued (for reviews see e.g. refs. [12, 13]) that, from the precise knowledge of the low-energy supersymmetric parameters one can shed light on the origin and mechanism of supersymmetry breaking and even on physics at much higher energies, like the GUT scale. The extrapolation of the supersymmetric parameters measured at the TeV energy scale to the GUT-scale raises inevitably the question of uncertainties involved. Currently, there are four publicly available spectrum generating codes [14 – 17] based on two-loop order MSSM renormalization group equations (RGEs) [18 – 21] subjected to two types of boundary conditions. One set of constraints accounts for the weak-scale matching between the MSSM and SM parameters to one-loop order [22]. The second one allows for the SUSY breaking at the high scale according to specific models like minimal supergravity, gauge mediation and anomaly mediation. The approximations within the codes differ by higher order corrections and by the treatment of the low-energy threshold corrections. The typical spread of the results is within few percents, which does not always meet the experimental accuracy [23]. Along the same line, recent analyses [24, 25] have proven that the three-loop order effects on the running of the strong coupling constant α_s and the bottom quark mass m_b may exceed those induced by the current experimental accuracy [26, 27].

Very recently, ref. [28] computed the two-loop SQCD and top-induced Supersymmetric Electroweak (SEW) corrections to the effective bottom Yukawa couplings. The knowledge of the two-loop corrections allows predictions for the branching ratios of the MSSM Higgs bosons with per-cent level accuracy.

The aim of this paper is to compute the weak-scale matching relations for the strong coupling constant and the bottom quark mass with two-loop accuracy, taking into account the exact dependence on the particle masses. This will extend the study of ref. [24] allowing phenomenological analyses based on quasi-realistic mass spectra for SUSY particles, with three-loop order accuracy. However, we will consider in this paper only the $\mathcal{O}(\alpha_s^2)$ corrections from SQCD and postpone the study of the SEW contributions $\mathcal{O}(\alpha_s y_t^2, \alpha_s y_b^2, y_t^4, y_t^2 y_b^2, y_b^4)$ to further investigations. Whereas the SEW corrections to the decoupling coefficient of α_s are expected to be negligible, their numerical impact on the running bottom quark mass can become as important as those from SQCD. At the one-loop order [22], the main contributions to the bottom-quark mass decoupling coefficient arise from diagrams containing gluino- and Higgsino-exchange. In the most regions of the MSSM parameter space the gluino contribution is the dominant one and can be as large as the tree-level bottom quark mass. However, there are domains in the parameter space where the corrections due to gluino- and Higgsino-exchange can become of the same order and have opposite sign. These regions contain the special points for which the Yukawa coupling unification occurs [11, 29]. For the MSSM parameters for which the radiative corrections to the bottom quark mass are comparable with the LO ones, ref. [30] proposed a method to resum them to all orders in perturbation theory. A numerical comparison with the results of ref. [30] can be found in section 5.

The paper is organized as follows: in section 2 and section 3 we discuss the theoretical framework and the renormalization scheme we use. In section 4 we present the

JHEP02(2009)037

analytical one- and two-loop results. The latter ones are displayed in analytical form for three simplifying mass hierarchies among the SUSY particles. The numerical effects are studied in section 5.

2. Framework

As already stated above, the underlying motivation for the running analysis is to relate physical parameters measured at the electroweak scale with the Lagrange parameters at the GUT scale. The running parameters are most conveniently defined in mass-independent renormalization schemes such as $\overline{\text{MS}}$ [31] for the SM parameters and $\overline{\text{DR}}$ [32] for the MSSM parameters. It is well known that in such "unphysical" renormalization schemes the Appelquist-Carazzone decoupling theorem [33] does not hold in its naive form. Quantum corrections to low-energy processes contain logarithmically enhanced contributions from heavy particles with masses much greater than the energy-scale of the process under consideration. An elegant approach to get rid of this unwanted behaviour in the $\overline{\text{MS}}$ or $\overline{\text{DR}}$ scheme is to formulate an effective theory (ET) [34, 35] integrating out all heavy particles. The coupling constants defined within the ET must be modified in order to account for the effects of the heavy fields. They are related to the parameters of the full theory by the so-called matching or decoupling relations.

For moderate mass splittings between SUSY particles, i.e. there are no large logarithms in the theory that have to be resummed by means of RGEs, the decoupling of heavy particles might be performed in one step [36]. The energy-scale at which the decoupling is performed is not fixed by the theory. It is usually chosen to be $\mu \simeq \tilde{M}$, where $\tilde{M}$ is a typical heavy particle mass. The MSSM parameters at energies $E \simeq \tilde{M}$ can be determined from the knowledge of the corresponding SM parameters and the associated decoupling relations.

The decoupling coefficients for the strong coupling constant and for the light quark masses are known in QCD with four- [37, 38] and three-loop [34] accuracy, respectively. Due to the presence of many mass scales, their computation within SQCD and SEW is quite involved. At one-loop order, they are known exactly [22, 39]. At two-loop order, the decoupling coefficient for the strong coupling is known only for specific mass hierarchies [24]. Recently, the two-loop SQCD corrections for the decoupling coefficient of the bottom-quark mass was computed [39]. The focus of this paper is the analytical computation of the decoupling relations for the strong coupling constant and the bottom-quark mass within SQCD through two-loops using a different method as ref. [39]. The comparison of the results will be discussed in the next section.

We consider SQCD with n_f active quark and $n_s = n_f$ active squark flavours and $n_{\tilde{g}} = 1$ gluinos. Furthermore, we assume that $n_l = 5$ quarks are light (among which the bottom quark) and that the top quark and all squarks and the gluino are heavy. Integrating out the heavy fields from the full SQCD Lagrangian, we obtain the Lagrange density corresponding to the effective QCD with n_l light quarks plus non-renormalizable interactions. The latter are suppressed by negative powers of the heavy masses and will be neglected here. The effective Lagrangian can be written as follows:

$$\mathcal{L}'(g_s^0, m_q^0, \xi^0; \psi_q^0, G_\mu^{0,a}, c^{0,a}; \zeta_i^0) = \mathcal{L}^{\text{SQCD}}(g_s^{0\prime}, m_q^{0\prime}, \xi^{0\prime}; \psi_q^{0\prime}, G_\mu^{0\prime,a}, c^{0\prime,a}), \tag{2.1}$$

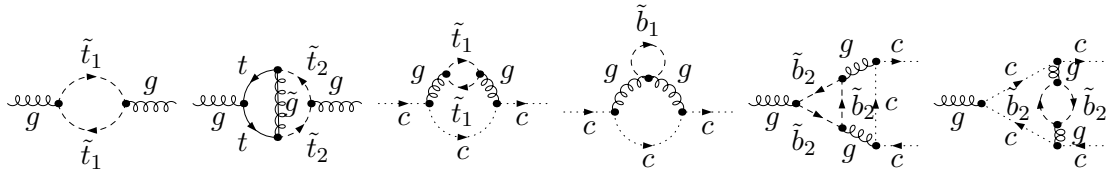

(a)

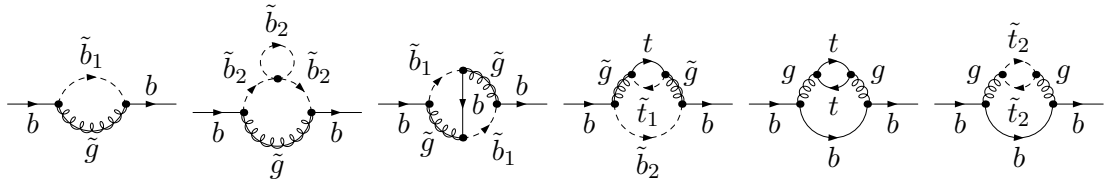

(b)

Figure 1: Sample diagrams contributing to ζ_3, $\tilde{\zeta}_3$, $\tilde{\zeta}_1$ and ζ_m with gluons (g), ghosts (c), bottom/top quarks (b/t), bottom/top squarks ($\tilde{b}/\tilde{t}$) and gluinos ($\tilde{g}$).

where ψ_q, G^a_μ, c^a denote the light-quark, the gluon and the ghost fields, respectively, m_q stands for the light quark masses, ξ is the gauge parameter and $g_s = \sqrt{4\pi\alpha_s}$ is the strong coupling. The index 0 marks bare quantities. $\mathcal{L}^{\rm SQCD}$ is the usual SQCD Lagrangian from which all heavy fields have been discarded. As a result the fields, masses and couplings associated with light particles have to be rescaled. They are labeled by a prime in eq. (2.1) and are related with the original parameters through decoupling relations:

$$\begin{aligned} g_s^{0\prime} &= \zeta_g^0 g_s^0\,, & m_q^{0\prime} &= \zeta_m^0 m_q^0\,, & \xi^{0\prime} - 1 &= \zeta_3^0(\xi^0 - 1)\,, \\ \psi_q^{0\prime} &= \sqrt{\zeta_2^0}\psi_q^0\,, & G_\mu^{0\prime,a} &= \sqrt{\zeta_3^0}G_\mu^{0,a}\,, & c^{0\prime,a} &= \sqrt{\tilde{\zeta}_3^0}c^{0,a}\,. \end{aligned} \tag{2.2}$$

Refs. [34] showed that the bare decoupling constants ζ_m^0, ζ_2^0, ζ_3^0, $\tilde{\zeta}_3^0$ can be derived from the quark, the gluon and the ghost propagators, all evaluated at vanishing external momenta. As a result, for calculations performed within the framework of Dimensional Regularization/Reduction (DREG/DRED) only the diagrams containing at least one heavy particle inside the loops do not vanish. In figure 1 are shown sample Feynman diagrams contributing to the decoupling coefficients for the strong coupling (a) and the bottom-quark mass (b).

For the computation of ζ_g one has to use the well-known Ward identities. A convenient choice is the relation:

$$\zeta_g^0 = \frac{\tilde{\zeta}_1^0}{\tilde{\zeta}_3^0\sqrt{\zeta_3^0}}\,, \tag{2.3}$$

where $\tilde{\zeta}_1^0$ denotes the decoupling constant for the ghost-gluon vertex.
The finite decoupling coefficients are obtained upon the renormalization of the bare pa-

JHEP02(2009)037

rameters. They are given by

$$\zeta_g = \frac{Z_g}{Z'_g}\zeta_g^0\,, \quad \zeta_m = \frac{Z_m}{Z'_m}\zeta_m^0\,, \tag{2.4}$$

where Z'_g and Z'_m correspond to the renormalization constants in the effective theory. Since we are interested in the two-loop results for ζ_i, $i = g, m$, the corresponding renormalization constants for SQCD and QCD have to be implemented with the same accuracy. Analytical results for them can be found in refs. [35, 20, 40].

As mentioned above, the decoupling coefficients can be related with vacuum integrals. The latter can be recursively reduced to a master-integral [41] using the method of integration by parts [42]. Given the large number of diagrams and occurrence of many different mass scales, we computed them with the help of an automated setup. The Feynman diagrams were generated with `QGRAF` [43] and further processed with `q2e` [44]. The reduction of various vacuum integrals to the master integral was performed by a self written `FORM` [45] routine. The reduction of topologies with two different massive and one massless lines requires a careful treatment. The related master integral can be easily derived from its general expression valid for massive lines, given in ref. [41].

3. Regularization and renormalization scheme

In our setup, we used the squark mass eigenstates and their mixing angles as input parameters. For convenience, we give below the relations between them and the parameters of the MSSM Lagrangian.

The squark mass eigenstates $\tilde{q}_{1,2}$ and their mass eigenvalues $m_{\tilde{q}_{1,2}}$ are obtained by diagonalizing the mass matrix

$$\mathcal{M}_{\tilde{q}} = \begin{pmatrix} M_L^2 & m_q X_q \\ m_q X_q & M_R^2 \end{pmatrix}\,, \tag{3.1}$$

where we used the notation

$$\begin{aligned} X_q &= A_q - \mu \begin{cases} \tan\beta\,, & \text{for down-type quarks} \\ \cot\beta\,, & \text{for up-type quarks} \end{cases}\,, \\ M_L^2 &= M_{\tilde{Q}}^2 + m_q^2 + M_Z^2(I_3^q - Q_q s_W^2)\cos 2\beta\,, \\ M_R^2 &= M_{\tilde{D},\tilde{U}}^2 + m_q^2 + M_Z^2 Q_q s_W^2 \cos 2\beta\,. \end{aligned} \tag{3.2}$$

Here m_q, I_3^q and Q_q are the mass, isospin and electric charge of the quark q, respectively, and $s_W = \sin\theta_W$. The parameters $M_{\tilde{Q}}$ and $M_{\tilde{D},\tilde{U}}$ are the soft supersymmetry breaking masses, A_q is a trilinear coupling and μ is the Higgs-Higgsino bilinear coupling.

The squark mass eigenvalues are defined through the unitary transformation

$$\begin{pmatrix} m_{\tilde{q}_1}^2 & 0 \\ 0 & m_{\tilde{q}_2}^2 \end{pmatrix} = \mathcal{R}_{\tilde{q}} \mathcal{M}_{\tilde{q}} \mathcal{R}_{\tilde{q}}^\dagger\,, \quad \text{with} \quad \mathcal{R}_{\tilde{q}} = \begin{pmatrix} \cos\theta_q & \sin\theta_q \\ -\sin\theta_q & \cos\theta_q \end{pmatrix}\,, \tag{3.3}$$

JHEP02(2009)037

and the squark mixing angle through

$$\sin 2\theta_q = \frac{2 m_q X_q}{m^2_{\tilde{q}_1} - m^2_{\tilde{q}_2}} \,. \tag{3.4}$$

Since we consider the two-loop $\mathcal{O}(\alpha_s^2)$ corrections, only the one-loop $\mathcal{O}(\alpha_s)$ counterterms for the input parameters are required. We have chosen the $\overline{\rm DR}$ scheme to renormalize the strong coupling constant, and the on-shell scheme for the masses of the heavy particles, i.e. the gluino, squarks and top quark. The corresponding one-loop renormalization constants are known analytically (see, e.g., ref. [22]). For the computation of the two-loop ζ_{m_b}, also the one-loop counterterm for the sbottom mixing angle θ_b is required. We adopted the on-shell renormalization prescription as defined in ref. [46]

$$\delta\theta_b = \frac{\mathrm{Re}\Sigma_{\tilde{b}_{12}}(m^2_{\tilde{b}_1}) + \mathrm{Re}\Sigma_{\tilde{b}_{12}}(m^2_{\tilde{b}_2})}{2(m^2_{\tilde{b}_1} - m^2_{\tilde{b}_2})} \,, \tag{3.5}$$

where $\Sigma_{\tilde{b}_{12}}$ is the non-diagonal on-shell sbottom self-energy.

As we neglect the bottom-quark mass w.r.t. heavy particle masses, an explicit dependence of the radiative corrections on m_b can occur only through bottom Yukawa couplings. In order to avoid the occurrence of large logarithms of the form $\alpha_s^2 \log(\mu^2/m_b^2)$ with $\mu \simeq \tilde{M}$, we have renormalized the bottom quark mass in the $\overline{\rm DR}$ scheme. In this way, the large logarithms are absorbed into the running mass and the higher order corrections are maintained small.

The renormalization prescription for the trilinear coupling A_b is fixed by the tree-level relation eq. (3.4), while the parameters $\mu_{\rm SUSY}$ and $\tan\beta$ do not acquire $\mathcal{O}(\alpha_s)$ corrections to the one-loop level. Generically, the counterterm for A_b can be expressed as

$$\delta A_b = \left(2\cos 2\theta_b \delta\theta_b + \sin 2\theta_b \frac{\delta m^2_{\tilde{b}_1} - \delta m^2_{\tilde{b}_2}}{m^2_{\tilde{b}_1} - m^2_{\tilde{b}_2}} - \sin 2\theta_b \frac{\delta m_b}{m_b} \right) \frac{m^2_{\tilde{b}_1} - m^2_{\tilde{b}_2}}{2 m_b} \,, \tag{3.6}$$

where δm_b and $\delta m^2_{\tilde{b}_{1,2}}$ are the counterterms corresponding to bottom-quark and squark masses, respectively. Due to the use of different renormalization prescriptions for the bottom/sbottom masses and mixing angle, the parameter A_b is renormalized in a *mixed* scheme.

For the regularization of ultra-violet divergencies, we have implemented DRED with the help of the so-called ϵ-scalars [47]. In softly broken SUSY theories, as it is the case of MSSM/SQCD, they get a radiatively induced mass. We choose to renormalize their mass in the on-shell scheme, requiring that the renormalized mass is equal to zero.

There are also other approaches available in the literature. We want to mention the one proposed in Ref [48], where the ϵ-scalars are treated as massive particles. This approach is known in the literature as the $\overline{\rm DR}'$ scheme. In this case, the ϵ-scalars have to be decoupled together with the heavy particles of the theory [39]. The advantage of this method is that it directly relates SQCD parameters regularized within DRED with those of QCD regularized within DREG, which are known from experiments. The price of this "shortcut" is on one hand, that additional diagrams containing the ϵ-scalars as massive particles occur in the

calculation of the decoupling coefficients. On the other hand, the contributions originating from the change of regularization scheme and those from the decoupling of heavy particles are not distinguishable anymore.

In our approach the change of regularization scheme from DRED to DREG has to be performed explicitly within QCD [19, 20, 49]. For our purposes, the two-loop conversion relations for the strong coupling constant and the bottom-quark mass are required. The complication that arises at this stage is the occurrence of the *evanescent coupling* α_e associated with the ϵ-scalar-quark-quark vertex. This has to be distinguished from the gauge coupling within non-supersymmetric theories (e.g. QCD). However, in SQCD they are identical with the gauge couplings, as required by SUSY. Using the ET procedure, we can relate them with the strong coupling within the full theory with the help of decoupling relations similar with those introduced in eq. (2.2)

$$\alpha_e' = \zeta_e \alpha_e = \zeta_e \alpha_s \,. \tag{3.7}$$

Following the method described above, one can calculate ζ_e evaluating the ϵ-scalar and quark-propagators and the ϵ-scalar-quark-quark vertex at vanishing external momentum. In ref. [25], its one-loop expression was computed under the simplifying assumption of a degenerate SUSY-mass spectrum. In principle, for our numerical analyses, that rely on solving a system of coupled differential equations involving also the evanescent coupling α_e, even the two-loop order corrections to ζ_e are needed. However, from the explicit calculation it turned out that the numerical effects induced by the two-loop corrections to ζ_e are below the per-mille level. For simplicity, we do not display the corresponding two-loop results in the following. The analytical formulae are available upon request from the authors.

The method outlined here and the one introduced in ref. [39] for the calculation of the decoupling coefficient of the bottom-quark mass are equivalent. This has to be understood in the usual sense, that the predictions for physical observables made in one scheme at a given order in perturbation theory can be translated to the other scheme through redefinitions of masses and couplings. We have explicitly checked implementing additionally the method of ref. [39] in our setup the equivalence property for the decoupling coefficient of the bottom-quark mass ζ_m through two-loop order. Apart from the obvious rescaling of the strong coupling and the bottom quark mass, also the sbottom masses have to be modified [48]

$$m_{\tilde{b}}^2|_{\overline{\rm DR}'} = m_{\tilde{b}}^2|_{\overline{\rm DR}} - \frac{\alpha_s^{\overline{\rm DR}}}{2\pi} C_F m_\epsilon^2 \,. \tag{3.8}$$

Here C_F is the Casimir invariant in the fundamental representation and m_ϵ denotes the mass of the ϵ-scalars. The indices $\overline{\rm DR}$ and $\overline{\rm DR}'$, respectively, specify the regularization scheme. We also compared numerically the results for the two-loop ζ_{m_b} obtained using our method with the ones depicted in figure 3 of ref. [39] and found very good agreement.

4. Analytical results

4.1 One-loop results

The exact one-loop results for the decoupling coefficients of the strong coupling constant ζ_s and bottom-quark mass ζ_m can be found in refs. [22, 39]. The analytical formula for ζ_e is new and we give it below up to $\mathcal{O}(\epsilon)$.

$$\begin{aligned}\zeta_s =& 1+\frac{\alpha_s^{(\mathrm{SQCD})}}{\pi}\Bigg[-\frac{1}{6}C_A L_{\tilde{g}}-\frac{1}{6}L_t-\sum_q\sum_{i=1,2}\frac{1}{24}L_{\tilde{q}_i}\\ &-\epsilon\bigg(\frac{C_A}{12}\big(L_{\tilde{g}}^2+\zeta(2)\big)+\frac{1}{12}\big(L_t^2+\zeta(2)\big)-\frac{1}{48}\sum_q\sum_{i=1,2}\big(L_{\tilde{q}_i}^2+\zeta(2)\big)\bigg)\Bigg], \quad (4.1)\\ \zeta_{e,q} =& 1+\frac{\alpha_s^{(\mathrm{SQCD})}}{\pi}\Bigg\{-T_F\frac{L_t}{2}+\frac{C_A}{4}\bigg(2+L_{\tilde{g}}+\sum_{i=1,2}(L_{\tilde{g}}-L_{\tilde{q}_i})\frac{m_{\tilde{q}_i}^2}{m_{\tilde{g}}^2-m_{\tilde{q}_1}^2}\bigg)\\ &+\frac{C_F}{4}\bigg(\sum_{i=1,2}\bigg(-1-2L_{\tilde{g}}+2L_{\tilde{q}_i}+(-L_{\tilde{g}}+L_{\tilde{q}_i})\frac{m_{\tilde{q}_i}^2}{m_{\tilde{g}}^2-m_{\tilde{q}_i}^2}\bigg)\frac{m_{\tilde{q}_i}^2}{m_{\tilde{g}}^2-m_{\tilde{q}_i}^2}\\ &+(-3-2L_{\tilde{g}})\bigg)+\epsilon\Bigg[-\frac{T_F}{4}\big(L_t^2+\zeta(2)\big)+\frac{C_A}{8}\bigg(4+4L_{\tilde{g}}+L_{\tilde{g}}^2+\zeta(2)+\\ &+\frac{1}{2}\sum_{i=1,2}(L_{\tilde{g}}-L_{\tilde{q}_i})(2+L_{\tilde{g}}+L_{\tilde{q}_i})\frac{m_{\tilde{q}_i}^2}{m_{\tilde{g}}^2-m_{\tilde{q}_i}^2}\bigg)+\frac{C_F}{8}\bigg(-7-6L_{\tilde{g}}-2L_{\tilde{g}}^2\\ &-2\zeta(2)+\frac{1}{2}\sum_{i=1,2}\bigg(-3-6L_{\tilde{g}}-2L_{\tilde{g}}^2+4L_{\tilde{q}_i}+2L_{\tilde{q}_i}^2\\ &-(L_{\tilde{g}}-L_{\tilde{q}_1})(3+L_{\tilde{g}}+L_{\tilde{q}_1})\frac{m_{\tilde{q}_i}^2}{m_{\tilde{g}}^2-m_{\tilde{q}_i}^2}\bigg)\frac{m_{\tilde{q}_i}^2}{m_{\tilde{g}}^2-m_{\tilde{q}_i}^2}\bigg)\Bigg]\Bigg\}, \quad (4.2)\\ \zeta_{m_b} =& 1+\frac{\alpha_s^{(\mathrm{SQCD})}}{\pi}C_F\sum_{i=1,2}\Bigg\{-\frac{(1+L_{\tilde{b}_i})}{4}\frac{m_{\tilde{b}_i}^2}{(m_{\tilde{b}_i}^2-m_{\tilde{g}}^2)}+\frac{(3+2L_{\tilde{b}_i})m_{\tilde{b}_i}^4-(3+2L_{\tilde{g}})m_{\tilde{g}}^4}{16(m_{\tilde{b}_i}^2-m_{\tilde{g}}^2)^2}\\ &-\frac{(-1)^i X_b m_{\tilde{g}}}{m_{\tilde{b}_1}^2-m_{\tilde{b}_2}^2}\frac{m_{\tilde{b}_i}^2L_{\tilde{b}_i}-m_{\tilde{g}}^2L_{\tilde{g}}}{2(m_{\tilde{b}_i}^2-m_{\tilde{g}}^2)}+\epsilon\Bigg[-\frac{m_{\tilde{b}_i}^2(2+L_{\tilde{b}_i}(2+L_{\tilde{b}_i})+\zeta(2))}{8(m_{\tilde{b}_i}^2-m_{\tilde{g}}^2)}\\ &+\frac{m_{\tilde{b}_i}^4(7+2L_{\tilde{b}_i}(3+L_{\tilde{b}_i})+2\zeta(2))-m_{\tilde{g}}^4(7+2L_{\tilde{g}}(3+L_{\tilde{g}})+2\zeta(2))}{32(m_{\tilde{b}_i}^2-m_{\tilde{g}}^2)^2}\\ &+\frac{(-1)^i X_b m_{\tilde{g}}}{m_{\tilde{b}_1}^2-m_{\tilde{b}_2}^2}\frac{m_{\tilde{g}}^2L_{\tilde{g}}(2+L_{\tilde{g}})-m_{\tilde{b}_i}^2L_{\tilde{b}_i}(2+L_{\tilde{b}_i})}{4(m_{\tilde{b}_i}^2-m_{\tilde{g}}^2)}\Bigg]\Bigg\}. \quad (4.3)\end{aligned}$$

In eqs. (4.1), (4.2), and (4.3), we have adopted the abbreviations

$$L_i=\ln\frac{\mu^2}{m_i^2}\,,\quad i\in\{t,\tilde{g},\tilde{q}_{1,2},\tilde{b}_{1,2}\}\,, \quad (4.4)$$

where $\tilde{q}_i(\tilde{b}_i)$ denote the super-partners of the quark $q(b)$. For our purposes, the special case $\zeta_{e,q=b}$ is of interest.

The colour factors are defined in case of a gauge group SU(N) as follows

$$C_F = \frac{N^2-1}{2N} \quad C_A = N\,, \quad T_F = \frac{1}{2}\,. \tag{4.5}$$

Furthermore, we used the notation $\zeta(2) = \pi^2/6$ and introduced the label "SQCD" to specify that the strong coupling has to be evaluated within the full theory, i.e. the SQCD with $n_f = n_s = 6$ active flavours.

The presence of the terms proportional with the parameter X_b is a manifestation of the supersymmetry breaking. They are generated by the Yukawa interaction between left- and right-handed bottom squarks and the CP-neutral Higgs fields. Their contribution to the decoupling coefficient of the bottom-quark mass can be related through the Low Energy Theorem [50] to the decay rate of the Higgs boson to $b\bar{b}$ pairs. To one-loop order, the X_b-term of eq. (4.3) coincides with the SQCD corrections to the decay rate $\phi \to b\bar{b}$ [51]. To higher orders, the relation between the two parameters becomes more involved.

The Yukawa-coupling induced contributions attracted a lot of attention in the past years, due to the fact that they are the dominant corrections for large values of $\tan\beta$. They may in general become comparable with the tree-level bottom-quark mass. The resummation of the one-loop corrections was performed in ref. [30].

4.2 Two-loop calculation

The analytical two-loop results for the decoupling coefficients are too lengthy to be displayed here. They are available in `MATHEMATICA` format from http://www-ttp.particle.uni-karlsruhe.de/Progdata/ttp08-25. Instead, we present the two-loop results for three special cases of the hierarchy among the heavy particle masses. Before displaying the analytical results, let us notice the absence of contributions of the form $\alpha_s^2 X_b^2$ to ζ_{m_b}, in accordance with refs. [30, 51]. They are suppressed by a factor $m_b/\tilde{M}$, that we neglect in the ET formalism.

4.2.1 Scenario A

We consider first the case of all supersymmetric particles having masses of the same order of magnitude and being much heavier than the top-quark

$$\begin{aligned} m_{\tilde{u}} = \cdots = m_{\tilde{b}} = m_{\tilde{t}} = m_{\tilde{g}} = \tilde{M} \quad &\gg \quad m_t \\ \alpha_s^{(5)} = \zeta_s^{\tilde{M}}\, \alpha_s^{(\mathrm{SQCD})}\,, \qquad & m_b^{(5)} = \zeta_{m_b}^{\tilde{M}}\, m_b^{(\mathrm{SQCD})}\,. \end{aligned}$$

$\zeta_s^{\tilde{M}}$, $\zeta_{m_b}^{\tilde{M}}$ are functions of the supersymmetric mass $\tilde{M}$ and the top-quark mass m_t, the soft SUSY breaking parameters X_q, $q = b, t$, the strong coupling constant in the full theory $\alpha_s^{(\mathrm{SQCD})}$ and the decoupling scale μ. The superscript (5) indicates that the parameters are defined in QCD with $n_l = 5$ light quarks. In addition to the notations introduced in eq. (4.4), the following abbreviation will be used

$$L_{\tilde{M}} = \ln \frac{\mu^2}{\tilde{M}^2}\,. \tag{4.6}$$

The two-loop result for the decoupling coefficient of α_s in case of a degenerate SUSY mass spectrum is known [24], however we give it here for completeness

$$\begin{aligned}
\zeta_s^{\tilde{M}} =& 1 + \frac{\alpha_s^{(\mathrm{SQCD})}}{\pi}\left[C_A\left(-\frac{1}{6}L_{\tilde{M}}\right) + \left(-L_{\tilde{M}} - \frac{L_t}{3}\right)T_F\right] + \left(\frac{\alpha_s^{(\mathrm{SQCD})}}{\pi}\right)^2\left\{C_A^2\left(-\frac{85}{288}\right.\right. \\
&- \frac{L_{\tilde{M}}}{3} + \frac{L_{\tilde{M}}^2}{36}\left.\right) + C_F T_F\left[-\frac{31}{16} - \frac{3L_{\tilde{M}}}{2} - \frac{L_t}{4} - \frac{m_t^2}{8\tilde{M}^2} + \frac{\pi m_t^3}{12\tilde{M}^3} + \left(-\frac{17}{150} - \frac{3L_{\tilde{M}}}{40}\right.\right. \\
&\left.\left.+ \frac{3L_t}{40}\right)\frac{m_t^4}{\tilde{M}^4}\right] + C_A T_F\left[\frac{41}{36} + L_{\tilde{M}} + \frac{L_{\tilde{M}}^2}{3} - \frac{5L_t}{12} + \frac{L_{\tilde{M}}L_t}{9} + \left(\frac{1}{8} + \frac{L_{\tilde{M}}}{4} - \frac{L_t}{4}\right)\frac{m_t^2}{m_S^2}\right. \\
&\left.- \frac{\pi m_t^3}{6\tilde{M}^3} + \left(\frac{19}{144} + \frac{L_{\tilde{M}}}{24} - \frac{L_t}{24}\right)\frac{m_t^4}{\tilde{M}^4}\right] + T_F^2\left(L_{\tilde{M}}^2 + \frac{2L_{\tilde{M}}L_t}{3} + \frac{L_t^2}{9}\right) \\
&\left.+ \mathcal{O}\left(\frac{m_t^5}{\tilde{M}^5}\right)\right\}, \qquad (4.7)
\end{aligned}$$

$$\begin{aligned}
\zeta_{m_b}^{\tilde{M}} =& 1 - \frac{\alpha_s^{(\mathrm{SQCD})}}{\pi}C_F\left[\frac{L_{\tilde{M}}}{4} + \frac{X_b}{4\tilde{M}}\right] + \left(\frac{\alpha_s^{(\mathrm{SQCD})}}{\pi}\right)^2 C_F\left\{-C_A\left(\frac{65}{1152} + \frac{43L_{\tilde{M}}}{96} + \frac{L_{\tilde{M}}^2}{32}\right)\right. \\
&+ C_F\left(-\frac{99}{128} - \frac{7L_{\tilde{M}}}{32} + \frac{L_{\tilde{M}}^2}{32}\right) + T_F\left[\frac{197}{72} - L_{\tilde{M}} + \frac{3L_{\tilde{M}}^2}{4} - \frac{L_t}{12} + \frac{L_t^2}{8}\right. \\
&\left.+ \left(\frac{7}{144} + \frac{L_{\tilde{M}}}{12} - \frac{L_t}{12}\right)\frac{m_t^2}{\tilde{M}^2} - \frac{\pi}{12}\frac{m_t^3}{\tilde{M}^3} + \left(\frac{53}{600} - \frac{7L_{\tilde{M}}}{160} + \frac{7L_t}{160}\right)\frac{m_t^4}{\tilde{M}^4}\right] \\
&+ \frac{X_b}{\tilde{M}}\left[-C_A\left(\frac{1}{16} + \frac{3L_{\tilde{M}}}{16}\right) - C_F\left(\frac{1}{4} - \frac{3L_{\tilde{M}}}{16}\right) + T_F\left[\frac{-3}{4} + \frac{3L_{\tilde{M}}}{4}\right.\right. \\
&\left.\left.+ \left(\frac{-7}{72} - \frac{L_{\tilde{M}}}{24} + \frac{L_t}{24}\right)\frac{m_t^2}{\tilde{M}^2} + \frac{\pi}{24}\frac{m_t^3}{\tilde{M}^3} + \left(-\frac{17}{450} + \frac{L_{\tilde{M}}}{240} - \frac{L_t}{240}\right)\frac{m_t^4}{\tilde{M}^4}\right]\right] \\
&+ \frac{X_t}{\tilde{M}}T_F\left[\left(\frac{-5}{72} + \frac{L_{\tilde{M}}}{12} - \frac{L_t}{12}\right)\frac{m_t^2}{\tilde{M}^2} - \frac{\pi}{24}\frac{m_t^3}{\tilde{M}^3} + \left(\frac{23}{450} - \frac{L_{\tilde{M}}}{60} + \frac{L_t}{60}\right)\frac{m_t^4}{\tilde{M}^4}\right] \\
&+ \frac{X_t X_b}{\tilde{M}^2}T_F\left[\left(\frac{1}{72} - \frac{L_{\tilde{M}}}{24} + \frac{L_t}{24}\right)\frac{m_t^2}{\tilde{M}^2} + \frac{\pi}{48}\frac{m_t^3}{\tilde{M}^3} + \left(\frac{-59}{1800} - \frac{L_{\tilde{M}}}{120} + \frac{L_t}{120}\right)\frac{m_t^4}{\tilde{M}^4}\right] \\
&\left.+ \mathcal{O}\left(\frac{m_t^5}{\tilde{M}^5}\right)\right\}. \qquad (4.8)
\end{aligned}$$

Let us point out that, according to eq. (3.4) the assumption of degenerate top-squark masses can be materialized only if $X_t \to 0$, due to the heavy top-quark mass. We display, however, for completeness the full result. Further on, the hypothesis of equal top- and bottom-squark masses is inconsistent with the SU(2) invariance of the $\tilde{t}/\tilde{b}$ isodublet imposed in models like mSUGRA.

4.2.2 Scenario B

In the following, we discuss the possibility that the gluino is the heaviest supersymmetric

particle and the squarks have equal masses, much heavier than that of the top-quark

$$m_{\tilde{g}} \quad \gg \quad m_{\tilde{u}} = \cdots = m_{\tilde{b}} = m_{\tilde{t}} = m_{\tilde{q}} \quad \gg \quad m_t$$
$$\alpha_s^{(5)} = \zeta_s^{\tilde{g}}\, \alpha_s^{(\mathrm{SQCD})}\,, \qquad m_b^{(5)} = \zeta_{m_b}^{\tilde{g}}\, m_b^{(\mathrm{SQCD})}\,.$$

The two-loop results read

$$\begin{aligned}
\zeta_s^{\tilde{g}} =& 1 + \frac{\alpha_s^{(\mathrm{SQCD})}}{\pi}\left[C_A\left(-\frac{1}{6}L_{\tilde{g}}\right) + \left(-\frac{L_t}{3} - L_{\tilde{q}}\right)T_F\right] + \left(\frac{\alpha_s^{(\mathrm{SQCD})}}{\pi}\right)^2\Bigg\{C_A^2\Bigg(-\frac{85}{288} - \frac{L_{\tilde{g}}}{3} \\
&+ \frac{L_{\tilde{g}}^2}{36}\Bigg) + T_F^2\left(\frac{L_t^2}{9} + \frac{2}{3}L_tL_{\tilde{q}} + L_{\tilde{q}}^2\right) + C_FT_F\Bigg[-\frac{19}{16} - \frac{L_t}{4} + \frac{3L_{\tilde{g}}}{2} - 3L_{\tilde{q}} + \left(\frac{1}{6} + L_{\tilde{g}}\right. \\
&\left. - L_{\tilde{q}}\right)\frac{m_{\tilde{q}}^2}{m_{\tilde{g}}^2} + \left(\frac{1}{24} + L_{\tilde{g}} - L_{\tilde{q}}\right)\frac{m_{\tilde{q}}^4}{m_{\tilde{g}}^4} + \left(-\frac{5}{9} + \frac{L_t}{3} - \frac{L_{\tilde{g}}}{3}\right)\frac{m_t^2}{m_{\tilde{g}}^2} + \left(-\frac{9}{8} + \frac{5L_t}{4} - \frac{5L_{\tilde{g}}}{4}\right)\frac{m_t^4}{m_{\tilde{g}}^4} \\
&+ \frac{m_t^2m_{\tilde{q}}^2}{m_{\tilde{g}}^4}\left(-\frac{41}{36} + \frac{11L_t}{6} - \frac{23L_{\tilde{g}}}{6} + L_tL_{\tilde{g}} - L_{\tilde{g}}^2 + 2L_{\tilde{q}} - L_tL_{\tilde{q}} + L_{\tilde{g}}L_{\tilde{q}} - 2\zeta_2\right)\Bigg] \\
&+ C_AT_F\Bigg[\frac{95}{36} - \frac{5L_t}{12} + \frac{3L_{\tilde{g}}}{2} + \frac{1}{9}L_tL_{\tilde{g}} - \frac{L_{\tilde{q}}}{2} + \frac{1}{3}L_{\tilde{g}}L_{\tilde{q}} + \left(-\frac{3L_{\tilde{g}}}{2} + \frac{3L_{\tilde{q}}}{2}\right)\frac{m_{\tilde{q}}^2}{m_{\tilde{g}}^2} \\
&+ \left(-\frac{3}{2} + \frac{3L_{\tilde{g}}}{2} - \frac{3L_{\tilde{q}}}{2}\right)\frac{m_{\tilde{q}}^4}{m_{\tilde{g}}^4} + \left(\frac{1}{2} - \frac{L_t}{4} + \frac{L_{\tilde{g}}}{4}\right)\frac{m_t^2}{m_{\tilde{g}}^2} + \left(\frac{1}{4} - \frac{L_t}{4} + \frac{L_{\tilde{g}}}{4}\right)\frac{m_t^4}{m_{\tilde{g}}^4} \\
&+ \frac{m_t^2m_{\tilde{q}}^2}{m_{\tilde{g}}^4}\left(\frac{1}{2} - \frac{3L_t}{4} + \frac{3L_{\tilde{g}}}{2} - \frac{1}{2}L_tL_{\tilde{g}} + \frac{L_{\tilde{g}}^2}{2} - \frac{3L_{\tilde{q}}}{4} + \frac{1}{2}L_tL_{\tilde{q}} - \frac{1}{2}L_{\tilde{g}}L_{\tilde{q}} + \zeta_2\right)\Bigg] \\
&+ \mathcal{O}\left(\frac{m_{\tilde{q}}^6}{m_{\tilde{g}}^6}, \frac{m_{\tilde{q}}^4m_t^2}{m_{\tilde{g}}^6}, \frac{m_{\tilde{q}}^2m_t^4}{m_{\tilde{g}}^6}, \frac{m_t^6}{m_{\tilde{g}}^6}\right)\Bigg\}, \qquad (4.9)
\end{aligned}$$

$$\begin{aligned}
\zeta_{m_b}^{\tilde{g}} =& 1 + \frac{\alpha_s^{(\mathrm{SQCD})}}{\pi}C_F\Bigg\{-\frac{3}{8} - \frac{L_{\tilde{g}}}{4} + \left(-\frac{1}{4} - \frac{L_{\tilde{g}}}{2} + \frac{L_{\tilde{q}}}{2}\right)\frac{m_{\tilde{q}}^2}{m_{\tilde{g}}^2} + \left(-\frac{1}{4} - \frac{3L_{\tilde{g}}}{4} + \frac{3L_{\tilde{q}}}{4}\right)\frac{m_{\tilde{q}}^4}{m_{\tilde{g}}^4} \\
&+ \frac{X_b}{m_{\tilde{g}}}\left[\frac{1}{2} + \frac{L_{\tilde{g}}}{2} - \frac{L_{\tilde{q}}}{2} + \left(\frac{1}{2} + L_{\tilde{g}} - L_{\tilde{q}}\right)\frac{m_{\tilde{q}}^2}{m_{\tilde{g}}^2} + \left(\frac{1}{2} + \frac{3L_{\tilde{g}}}{2} - \frac{3L_{\tilde{q}}}{2}\right)\frac{m_{\tilde{q}}^4}{m_{\tilde{g}}^4}\right]\Bigg\} \\
&+ \left(\frac{\alpha_s^{(\mathrm{SQCD})}}{\pi}\right)^2 C_F\Bigg\{C_A\Bigg[-\frac{209}{1152} - \frac{35L_{\tilde{g}}}{48} - \frac{L_{\tilde{g}}^2}{32} - \frac{\zeta(2)}{8} + \left(-\frac{5}{16} - \frac{3L_{\tilde{g}}}{2} - \frac{5L_{\tilde{g}}^2}{8}\right. \\
&\left. + \frac{21L_{\tilde{q}}}{16} + \frac{7L_{\tilde{g}}L_{\tilde{q}}}{8} - \frac{L_{\tilde{q}}^2}{4} - \frac{5\zeta(2)}{8}\right)\frac{m_{\tilde{q}}^2}{m_{\tilde{g}}^2} + \left(\frac{7}{32} - \frac{11L_{\tilde{g}}}{4} - \frac{37L_{\tilde{g}}^2}{32} + \frac{41L_{\tilde{q}}}{16} + \frac{7L_{\tilde{g}}L_{\tilde{q}}}{4} - \frac{19L_{\tilde{q}}^2}{32}\right. \\
&\left. - \frac{5\zeta(2)}{8}\right)\frac{m_{\tilde{q}}^4}{m_{\tilde{g}}^4}\Bigg] + C_F\Bigg[-\frac{221}{128} - \frac{L_{\tilde{g}}}{8} + \frac{L_{\tilde{g}}^2}{32} - \frac{\zeta(2)}{16} + \left(\frac{9}{16} + \frac{5L_{\tilde{g}}^2}{8} + \frac{L_{\tilde{q}}}{16} - \frac{9L_{\tilde{g}}L_{\tilde{q}}}{8}\right. \\
&\left. + \frac{L_{\tilde{q}}^2}{2} + \frac{\zeta(2)}{2}\right)\frac{m_{\tilde{q}}^2}{m_{\tilde{g}}^2} + \left(\frac{31}{192} + \frac{35L_{\tilde{g}}}{32} + \frac{17L_{\tilde{g}}^2}{16} - \frac{33L_{\tilde{q}}}{32} - \frac{31L_{\tilde{g}}L_{\tilde{q}}}{16} + \frac{7L_{\tilde{q}}^2}{8} + \frac{\zeta(2)}{8}\right)\frac{m_{\tilde{q}}^4}{m_{\tilde{g}}^4}\Bigg] \\
&+ T_F\Bigg[\frac{139}{36} + \frac{3L_{\tilde{g}}}{2} + \frac{3L_{\tilde{g}}^2}{8} - \frac{11L_{\tilde{q}}}{8} + \frac{3L_{\tilde{q}}^2}{8} - \frac{L_t}{12} + \frac{L_t^2}{8} + \frac{3\zeta(2)}{4}
\end{aligned}$$

JHEP02(2009)037

$$
+\left(3+\frac{9L_{\tilde{g}}}{2}+3L_{\tilde{g}}^2-\frac{15L_{\tilde{q}}}{4}-\frac{9L_{\tilde{g}}L_{\tilde{q}}}{2}+\frac{3L_{\tilde{q}}^2}{2}\right)\frac{m_{\tilde{q}}^2}{m_{\tilde{g}}^2}+\left(-\frac{1}{2}-\frac{L_{\tilde{g}}}{4}+\frac{L_{\tilde{q}}}{4}\right)\frac{m_t^2}{m_{\tilde{g}}^2}
$$

$$
-\left(1+\frac{L_{\tilde{g}}}{2}-\frac{3L_{\tilde{g}}^2}{8}-\frac{L_{\tilde{q}}}{2}+\frac{3L_{\tilde{g}}L_{\tilde{q}}}{4}-\frac{3L_{\tilde{q}}^2}{8}-\frac{3\zeta(2)}{4}\right)\frac{m_{\tilde{q}}^2m_t^2}{m_{\tilde{g}}^4}
$$

$$
+\left(-\frac{5}{72}+\frac{L_{\tilde{q}}}{24}-\frac{L_t}{24}\right)\frac{m_t^4}{m_{\tilde{q}}^2m_{\tilde{g}}^2}+\left(-\frac{155}{96}-\frac{3L_{\tilde{g}}}{16}+\frac{3L_{\tilde{g}}^2}{16}+\frac{7L_{\tilde{q}}}{8}-\frac{3L_{\tilde{q}}^2}{16}-\frac{11L_t}{16}\right.
$$

$$
\left.-\frac{3L_{\tilde{g}}L_t}{8}+\frac{3L_{\tilde{q}}L_t}{8}+\frac{3\zeta(2)}{8}\right)\frac{m_t^4}{m_{\tilde{g}}^4}+\left(\frac{69}{16}+\frac{63L_{\tilde{g}}}{8}+3L_{\tilde{g}}^2-\frac{57L_{\tilde{q}}}{8}-\frac{15L_{\tilde{g}}L_{\tilde{q}}}{4}+\frac{3L_{\tilde{q}}^2}{4}\right)\frac{m_{\tilde{q}}^4}{m_{\tilde{g}}^4}\Bigg]
$$

$$
+\frac{X_b}{m_{\tilde{g}}}\Bigg[C_A\Bigg[\frac{7}{8}+L_{\tilde{g}}+\frac{3L_{\tilde{g}}^2}{8}-\frac{5L_{\tilde{q}}}{8}-\frac{3L_{\tilde{g}}L_{\tilde{q}}}{8}-\frac{\zeta(2)}{4}+\left(\frac{9}{8}+\frac{17L_{\tilde{g}}}{8}+\frac{11L_{\tilde{g}}^2}{8}-\frac{7L_{\tilde{q}}}{4}\right.
$$

$$
\left.-2L_{\tilde{g}}L_{\tilde{q}}+\frac{5L_{\tilde{q}}^2}{8}-\frac{\zeta(2)}{4}\right)\frac{m_{\tilde{q}}^2}{m_{\tilde{g}}^2}+\left(\frac{19}{16}+\frac{27L_{\tilde{g}}}{8}+\frac{23L_{\tilde{g}}^2}{8}-3L_{\tilde{q}}-\frac{37L_{\tilde{g}}L_{\tilde{q}}}{8}+\frac{7L_{\tilde{q}}^2}{4}\right.
$$

$$
\left.-\frac{\zeta(2)}{4}\right)\frac{m_{\tilde{q}}^4}{m_{\tilde{g}}^4}\Bigg]+C_F\Bigg[\frac{1}{16}-\frac{3L_{\tilde{g}}}{16}-\frac{3L_{\tilde{g}}^2}{8}-\frac{3L_{\tilde{q}}}{16}+\frac{3L_{\tilde{g}}L_{\tilde{q}}}{8}+\frac{\zeta(2)}{2}+\left(-\frac{9}{16}-\frac{5L_{\tilde{g}}}{24}\right.
$$

$$
\left.-\frac{3L_{\tilde{g}}^2}{2}-\frac{L_{\tilde{q}}}{6}+\frac{9L_{\tilde{g}}L_{\tilde{q}}}{4}-\frac{3L_{\tilde{q}}^2}{4}+\frac{\zeta(2)}{2}\right)\frac{m_{\tilde{q}}^2}{m_{\tilde{g}}^2}+\left(-\frac{13}{16}-\frac{3L_{\tilde{g}}}{4}-\frac{13L_{\tilde{g}}^2}{4}+\frac{3L_{\tilde{q}}}{8}\right.
$$

$$
\left.+\frac{43L_{\tilde{g}}L_{\tilde{q}}}{8}-\frac{17L_{\tilde{q}}^2}{8}+\frac{\zeta(2)}{2}\right)\frac{m_{\tilde{q}}^4}{m_{\tilde{g}}^4}\Bigg]+T_F\Bigg[-\frac{3}{2}(2+L_{\tilde{g}})(1+L_{\tilde{g}}-L_{\tilde{q}})+\left(-9-\frac{15L_{\tilde{g}}}{2}\right.
$$

$$
\left.-6L_{\tilde{g}}^2+6L_{\tilde{q}}+9L_{\tilde{g}}L_{\tilde{q}}-3L_{\tilde{q}}^2\right)\frac{m_{\tilde{q}}^2}{m_{\tilde{g}}^2}+\left(\frac{3}{2}+\frac{L_{\tilde{g}}}{2}-\frac{L_{\tilde{q}}}{2}\right)\frac{m_t^2}{m_{\tilde{g}}^2}+\left(-\frac{33}{4}-\frac{63L_{\tilde{g}}}{4}-6L_{\tilde{g}}^2\right.
$$

$$
\left.+\frac{57L_{\tilde{q}}}{4}+\frac{15L_{\tilde{g}}L_{\tilde{q}}}{2}-\frac{3L_{\tilde{q}}^2}{2}\right)\frac{m_{\tilde{q}}^4}{m_{\tilde{g}}^4}+\left(\frac{5}{18}-\frac{L_{\tilde{q}}}{6}+\frac{L_t}{6}\right)\frac{m_t^4}{m_{\tilde{q}}^2m_{\tilde{g}}^2}
$$

$$
+\left(\frac{5}{2}+\frac{3L_{\tilde{g}}}{2}-\frac{L_{\tilde{g}}^2}{2}-\frac{3L_{\tilde{q}}}{2}+L_{\tilde{g}}L_{\tilde{q}}-\frac{L_{\tilde{q}}^2}{2}-2\zeta(2)\right)\frac{m_t^2m_{\tilde{q}}^2}{m_{\tilde{g}}^4}
$$

$$
+\left(\frac{301}{72}+\frac{5L_{\tilde{g}}}{8}-\frac{L_{\tilde{g}}^2}{4}-\frac{53L_{\tilde{q}}}{24}-\frac{L_{\tilde{g}}L_{\tilde{q}}}{4}+\frac{L_{\tilde{q}}^2}{2}+\frac{19L_t}{12}+\frac{3L_{\tilde{g}}L_t}{4}-\frac{3L_{\tilde{q}}L_t}{4}-\zeta(2)\right)\frac{m_t^4}{m_{\tilde{g}}^4}\Bigg]\Bigg]
$$

$$
+\frac{X_t}{m_{\tilde{g}}}T_F\Bigg[\left(\frac{1}{2}-L_{\tilde{g}}-\frac{L_{\tilde{g}}^2}{4}+L_{\tilde{q}}+\frac{L_{\tilde{g}}L_{\tilde{q}}}{2}-\frac{L_{\tilde{q}}^2}{4}-\frac{\zeta(2)}{2}\right)\frac{m_t^2}{m_{\tilde{g}}^2}+\left(1-\frac{7L_{\tilde{g}}}{2}-2L_{\tilde{g}}^2+\frac{7L_{\tilde{q}}}{2}\right.
$$

$$
\left.+4L_{\tilde{g}}L_{\tilde{q}}-2L_{\tilde{q}}^2-2\zeta(2)\right)\frac{m_t^2m_{\tilde{q}}^2}{m_{\tilde{g}}^4}+\left(\frac{4}{9}-\frac{L_{\tilde{q}}}{6}+\frac{L_t}{6}\right)\frac{m_t^4}{m_{\tilde{g}}^2m_{\tilde{q}}^2}+\left(\frac{17}{9}-3L_{\tilde{g}}-L_{\tilde{g}}^2+\frac{L_{\tilde{q}}}{6}\right.
$$

$$
\left.+L_{\tilde{g}}L_{\tilde{q}}+\frac{17L_t}{6}+L_{\tilde{g}}L_t-L_{\tilde{q}}L_t-2\zeta(2)\right)\frac{m_t^4}{m_{\tilde{g}}^4}\Bigg]+\frac{X_tX_b}{m_{\tilde{g}}^2}T_F\Bigg[-\frac{1}{2}\frac{m_t^2}{m_{\tilde{q}}^2}+\left(-\frac{3}{2}+\frac{5L_{\tilde{g}}}{2}\right.
$$

$$
\left.+\frac{5L_{\tilde{g}}^2}{4}-\frac{5L_{\tilde{q}}}{2}-\frac{5L_{\tilde{g}}L_{\tilde{q}}}{2}+\frac{5L_{\tilde{q}}^2}{4}+\frac{3\zeta(2)}{2}\right)\frac{m_t^2}{m_{\tilde{g}}^2}\Bigg]+\mathcal{O}\left(\frac{m_{\tilde{q}}^6}{m_{\tilde{g}}^6},\frac{m_{\tilde{q}}^4m_t^2}{m_{\tilde{g}}^6},\frac{m_{\tilde{q}}^2m_t^4}{m_{\tilde{g}}^6},\frac{m_t^6}{m_{\tilde{g}}^6},\frac{X_tX_bm_t^4}{m_{\tilde{g}}^6}\right)\Bigg\}. \tag{4.10}
$$

4.2.3 Scenario C

Finally, we make the assumption that all squark masses are degenerate and are much

JHEP02(2009)037

heavier than the gluino and top masses

$$m_{\tilde{u}} = \cdots = m_{\tilde{b}} = m_{\tilde{t}} = m_{\tilde{q}} \quad \gg \quad m_{\tilde{g}} \quad \gg \quad m_t$$
$$\alpha_s^{(5)} = \zeta_s^{\tilde{q}}\, \alpha_s^{(\mathrm{SQCD})}\,, \qquad m_b^{(5)} = \zeta_{m_b}^{\tilde{q}}\, m_b^{(\mathrm{SQCD})}\,.$$

The decoupling coefficients are given by

$$\begin{aligned}
\zeta_s^{\tilde{q}} &= 1 + \frac{\alpha_s^{(\mathrm{SQCD})}}{\pi}\bigg[-\frac{1}{6}C_A L_{\tilde{g}} + \bigg(-\frac{L_t}{3} - L_{\tilde{q}}\bigg)T_F\bigg] + \bigg(\frac{\alpha_s^{(\mathrm{SQCD})}}{\pi}\bigg)^2 \bigg\{ C_A^2 \bigg(-\frac{85}{288} - \frac{L_{\tilde{g}}}{3} \\
&\quad + \frac{L_{\tilde{g}}^2}{36}\bigg) + C_F T_F \bigg[-\frac{7}{16} - \frac{L_t}{4} - \frac{3L_{\tilde{q}}}{2} + \bigg(-\frac{1}{9} - \frac{L_t}{12} + \frac{L_{\tilde{q}}}{12}\bigg)\frac{m_t^4}{m_{\tilde{q}}^4} + \bigg(-\frac{1}{9} - \frac{L_t}{3} \\
&\quad + \frac{L_{\tilde{q}}}{3}\bigg)\frac{m_t^2 m_{\tilde{g}}^2}{m_{\tilde{q}}^4} + \bigg(-\frac{3}{4} - \frac{3L_{\tilde{g}}}{2} + \frac{3L_{\tilde{q}}}{2}\bigg)\frac{m_{\tilde{g}}^4}{m_{\tilde{q}}^4} + \bigg(\frac{1}{18} + \frac{L_t}{6} - \frac{L_{\tilde{q}}}{6}\bigg)\frac{m_t^2}{m_{\tilde{q}}^2}\bigg] + T_F^2\bigg(\frac{L_t^2}{9} \\
&\quad + \frac{2}{3}L_t L_{\tilde{q}} + L_{\tilde{q}}^2\bigg) + C_A T_F \bigg[\frac{41}{36} - \frac{5L_t}{12} + \frac{1}{9}L_t L_{\tilde{g}} + L_{\tilde{q}} + \frac{1}{3}L_{\tilde{g}} L_{\tilde{q}} + \bigg(-\frac{L_t}{4} + \frac{L_{\tilde{q}}}{4}\bigg)\frac{m_t^2}{m_{\tilde{q}}^2} \\
&\quad + \bigg(\frac{1}{3} - \frac{L_{\tilde{g}}}{2} + \frac{L_{\tilde{q}}}{2}\bigg)\frac{m_{\tilde{g}}^2}{m_{\tilde{q}}^2} + \bigg(-\frac{L_t}{4} + \frac{L_{\tilde{q}}}{4}\bigg)\frac{m_t^4}{m_{\tilde{q}}^4} + \bigg(\frac{1}{12} - \frac{L_{\tilde{g}}}{2} + \frac{L_{\tilde{q}}}{2}\bigg)\frac{m_{\tilde{g}}^4}{m_{\tilde{q}}^4} \\
&\quad + \frac{m_t^2 m_{\tilde{g}}^2}{m_{\tilde{q}}^4}\bigg(\frac{7}{18} - \frac{3L_t}{4} - \frac{13L_{\tilde{g}}}{12} + \frac{1}{2}L_t L_{\tilde{g}} + \frac{11L_{\tilde{q}}}{6} - \frac{1}{2}L_t L_{\tilde{q}} - \frac{1}{2}L_{\tilde{g}} L_{\tilde{q}} + \frac{L_{\tilde{q}}^2}{2} + \zeta_2\bigg)\bigg] \\
&\quad + \mathcal{O}\bigg(\frac{m_{\tilde{g}}^6}{m_{\tilde{q}}^6}, \frac{m_{\tilde{g}}^4 m_t^2}{m_{\tilde{q}}^6}, \frac{m_{\tilde{g}}^2 m_t^4}{m_{\tilde{q}}^6}, \frac{m_t^6}{m_{\tilde{q}}^6}\bigg)\bigg\}, \qquad (4.11) \\
\zeta_{m_b}^{\tilde{q}} &= 1 + \frac{\alpha_s^{(\mathrm{SQCD})}}{\pi} C_F \bigg\{ -\frac{1}{8} - \frac{L_{\tilde{q}}}{4} + \frac{m_{\tilde{g}}^2}{4m_{\tilde{q}}^2} + \bigg(\frac{1}{4} - \frac{L_{\tilde{g}}}{4} + \frac{L_{\tilde{q}}}{4}\bigg)\frac{m_{\tilde{g}}^4}{m_{\tilde{q}}^4} + \frac{X_b}{m_{\tilde{q}}}\bigg[-\frac{m_{\tilde{g}}}{2m_{\tilde{q}}} \\
&\quad + \bigg(-\frac{1}{2} + \frac{L_{\tilde{g}}}{2} - \frac{L_{\tilde{q}}}{2}\bigg)\frac{m_{\tilde{g}}^3}{m_{\tilde{q}}^3}\bigg]\bigg\} + \bigg(\frac{\alpha_s^{(\mathrm{SQCD})}}{\pi}\bigg)^2 C_F \bigg\{ C_A \bigg[\frac{295}{1152} - \frac{L_{\tilde{g}}}{24} + \frac{L_{\tilde{g}}^2}{16} - \frac{L_{\tilde{q}}}{2} - \frac{3L_{\tilde{q}}^2}{32} \\
&\quad - \frac{\zeta(2)}{2} + \bigg(\frac{15}{16} + \frac{L_{\tilde{g}}}{2} - \frac{5L_{\tilde{q}}}{16} - \frac{5\zeta(2)}{8}\bigg)\frac{m_{\tilde{g}}^2}{m_{\tilde{q}}^2} + \bigg(\frac{19}{16} + \frac{3L_{\tilde{g}}}{16} + \frac{7L_{\tilde{g}}^2}{32} + \frac{13L_{\tilde{q}}^2}{32} - \frac{5L_{\tilde{g}} L_{\tilde{q}}}{8} \\
&\quad - \frac{5\zeta(2)}{8}\bigg)\frac{m_{\tilde{g}}^4}{m_{\tilde{q}}^4}\bigg] + C_F \bigg[-\frac{205}{128} - \frac{3L_{\tilde{q}}}{16} + \frac{L_{\tilde{q}}^2}{32} + \frac{15\zeta(2)}{16} + \bigg(-\frac{3}{2} - \frac{L_{\tilde{q}}}{16} + \frac{5\zeta(2)}{4}\bigg)\frac{m_{\tilde{g}}^2}{m_{\tilde{q}}^2} \\
&\quad + \bigg(-\frac{187}{64} - \frac{39L_{\tilde{g}}}{32} - \frac{7L_{\tilde{g}}^2}{8} + \frac{37L_{\tilde{q}}}{32} + \frac{29L_{\tilde{q}} L_{\tilde{g}}}{16} - \frac{15L_{\tilde{q}}^2}{16} + \frac{13\zeta(2)}{8}\bigg)\frac{m_{\tilde{g}}^4}{m_{\tilde{q}}^4}\bigg] \\
&\quad + T_F \bigg[\frac{28}{9} - \frac{L_t}{12} + \frac{L_t^2}{8} - \frac{5L_{\tilde{q}}}{8} + \frac{3L_{\tilde{q}}^2}{4} - \frac{3\zeta(2)}{4} + \bigg(\frac{3}{4} - \frac{3L_{\tilde{q}}}{4}\bigg)\frac{m_{\tilde{g}}^2}{m_{\tilde{q}}^2} + \bigg(-\frac{1}{2} + \frac{\zeta(2)}{4}\bigg)\frac{m_t^2}{m_{\tilde{q}}^2} \\
&\quad + \bigg(-\frac{13}{16} + \frac{3L_{\tilde{g}}}{8} - \frac{9L_{\tilde{q}}}{8} + \frac{3L_{\tilde{g}} L_{\tilde{q}}}{4} - \frac{3L_{\tilde{q}}^2}{4}\bigg)\frac{m_{\tilde{g}}^4}{m_{\tilde{q}}^4} + \bigg(-\frac{5}{2} + \frac{3\zeta(2)}{2}\bigg)\frac{m_t^2 m_{\tilde{g}}^2}{m_{\tilde{q}}^4} \\
&\quad + \bigg(\frac{61}{288} - \frac{\zeta(2)}{8} + \frac{L_t}{48} - \frac{L_{\tilde{q}}}{48}\bigg)\frac{m_t^4}{m_{\tilde{q}}^4}\bigg] + \frac{X_b}{m_{\tilde{q}}}\bigg[C_A \bigg[\bigg(-\frac{7}{8} + \frac{3L_{\tilde{g}}}{8} - \frac{3L_{\tilde{q}}}{4} - \frac{\zeta(2)}{4}\bigg)\frac{m_{\tilde{g}}}{m_{\tilde{q}}}
\end{aligned}$$

JHEP02(2009)037

$$
+\Big(-\frac{5}{8}+2L_{\tilde g}-\frac{19L_{\tilde q}}{8}+\frac{3L_{\tilde g}L_{\tilde q}}{8}-\frac{3L_{\tilde q}^2}{8}-\frac{\zeta(2)}{4}\Big)\frac{m_{\tilde g}^3}{m_{\tilde q}^3}\Big]+C_F\Big[\Big(-\frac{3}{16}+\frac{3L_{\tilde q}}{8}
$$

$$
+\frac{\zeta(2)}{2}\Big)\frac{m_{\tilde g}}{m_{\tilde q}}+\Big(-\frac{13}{16}-\frac{13L_{\tilde g}}{16}+\frac{19L_{\tilde q}}{16}-\frac{3L_{\tilde g}L_{\tilde q}}{8}+\frac{3L_{\tilde q}^2}{8}+\frac{\zeta(2)}{2}\Big)\frac{m_{\tilde g}^3}{m_{\tilde q}^3}\Big]
$$

$$
+T_F\Big[\Big(-\frac{3}{4}+\frac{3L_{\tilde q}}{2}\Big)\frac{m_{\tilde g}}{m_{\tilde q}}+\Big(\frac{7}{4}-\frac{3L_{\tilde g}}{4}+\frac{9L_{\tilde q}}{4}-\frac{3L_{\tilde g}L_{\tilde q}}{2}+\frac{3L_{\tilde q}^2}{2}\Big)\frac{m_{\tilde g}^3}{m_{\tilde q}^3}
$$

$$
+\Big(\frac{13}{4}-2\zeta(2)\Big)\frac{m_t^2m_{\tilde g}}{m_{\tilde q}^3}\Big]\Big]-\frac{X_t}{m_{\tilde q}}T_F\frac{\zeta(2)}{2}\frac{m_t^2m_{\tilde g}}{m_{\tilde q}^3}+\frac{X_tX_b}{m_{\tilde q}^2}T_F\Big[\frac{\zeta(2)}{2}\frac{m_t^2}{m_{\tilde q}^2}
$$

$$
+\Big(\frac{3}{4}-3L_{\tilde g}+3L_{\tilde q}+3\zeta(2)\Big)\frac{m_t^2m_{\tilde g}^2}{m_{\tilde q}^4}+\Big(\frac{5}{9}-\frac{2L_t}{3}+\frac{2L_{\tilde q}}{3}\Big)\frac{m_t^4}{m_{\tilde q}^4}\Big]
$$

$$
+\mathcal{O}\Big(\frac{m_{\tilde g}^6}{m_{\tilde q}^6},\frac{m_{\tilde g}^4m_t^2}{m_{\tilde q}^6},\frac{m_{\tilde g}^2m_t^4}{m_{\tilde q}^6},\frac{m_t^6}{m_{\tilde q}^6},\frac{X_bm_{\tilde g}^5}{m_{\tilde q}^6},\frac{X_tm_{\tilde g}^5}{m_{\tilde q}^6}\Big)\Big\}\,. \tag{4.12}
$$

We displayed in the previous expressions only the first three terms of the Taylor expansions in the mass ratios. To get an idea about the convergence of the perturbative series we fix the following input parameters: $m_t = 172.4\,\text{GeV}$, $\alpha_s^{(\text{SQCD})} = 0.120$, $m_{\tilde q} = 500\,\text{GeV}$, $X_q = -4000\,\text{GeV}$, $X_t = -400\,\text{GeV}$ and let $m_{\tilde g}$ vary. Even for $m_{\tilde g}/m_{\tilde q} = 0.5$, and 2 the approximations given above agree with the exact results with an accuracy better than 1%. For the case of degenerate SUSY masses, *i.e.* $m_{\tilde g}/m_{\tilde q} = 1$ the accuracy is even below the per-mille level.

5. Numerical results

In this section we discuss the numerical impact of the two-loop calculations we presented above. A first phenomenological application is the prediction of the strong coupling and the running bottom-quark mass at high-energy scales like $\tilde M = 1\,\text{TeV}$ or $\mu_{\text{GUT}} = 10^{16}\,\text{GeV}$, starting from their low-energy values determined experimentally.

For the energy evolution of the two parameters, we follow the method proposed in ref. [25]: first, we compute $\alpha_s^{(5)}(\mu_{\text{dec}})$ and $m_b^{(5)}(\mu_{\text{dec}})$ from $\alpha_s^{(5)}(M_Z)$ and $m_b^{(5)}(m_b)$, respectively, using the corresponding i-loop SM RGEs [35]. Here μ_{dec} denotes the energy scale at which the heavy particles are supposed to become active, i.e. the scale where the matching between the SM and the MSSM is performed. As pointed out in previous works [36], one can avoid part of the complications related with the occurrence of the *evanescent couplings*, performing the change of the regularization scheme from the $\overline{\text{MS}}$ to the $\overline{\text{DR}}$ scheme at the same scale. Nevertheless, one cannot avoid the occurrence of the evanescent coupling α_e in the $\overline{\text{MS}}$-$\overline{\text{DR}}$ relation for the bottom-quark mass. It has to be determined iteratively from the knowledge of the strong coupling at the matching scale. For consistency, the i-loop running parameters have to be folded with $(i-1)$-loop conversion and decoupling relations. Above the decoupling scale, the energy dependence of the running parameters is governed by the i-loop MSSM RGEs [36]. We solved numerically the system of coupled differential equations arising from the two sets of RGEs, and implemented this procedure for $i = 1, 2, 3$.

JHEP02(2009)037

The decoupling scale is not a physical parameter and cannot be predicted by the theory. It is usually chosen to be of the order of the heavy particle mass in order to circumvent the appearance of large logarithms. At fixed order perturbation theory, it is expected that the relations between the running parameters evaluated at high-energy scales and their low-energy values become less sensitive to the choice of $\mu_{\rm dec}$ once higher order radiative corrections are considered. The dependence on the precise value of the decoupling scale is interpreted as a measure of the unknown higher order corrections. We discuss the scale dependence of $\alpha_s(\mu_{\rm GUT})$ and $m_b(\mu_{\rm GUT})$ in figure 2 and figure 3, respectively.

For the SM parameters we used $\alpha_s(M_Z) = 0.1189$ [26], where $M_Z = 91.1876$ GeV [52], $m_b(\mu_b) = 4.164\,\text{GeV}$ [27], with $\mu_b = m_b(\mu_b)$, and $M_t = 172.4$ GeV [53]. For the SQCD parameters, we implemented their values for the SPS1a′ scenario [13]: $m_{\tilde{g}} = 607.1\,\text{GeV}$, $m_{\tilde{t}_1} = 366.5\,\text{GeV}$, $m_{\tilde{t}_2} = 585.5\,\text{GeV}$, $m_{\tilde{b}_1} = 506.3\,\text{GeV}$, $m_{\tilde{b}_2} = 545.7\,\text{GeV}$, $A_t^{\overline{\rm DR}}(1\text{ TeV}) = -565.1\,\text{GeV}$, $A_b^{\overline{\rm DR}}(1\text{ TeV}) = -943.4\,\text{GeV}$, $\mu = 396.0\,\text{GeV}$, and $\tan\beta = 10.0$.

For the calculation of ζ_{m_b} to two-loop accuracy, the $\overline{\rm DR}$ parameter A_b has to be converted to the renormalization scheme we used here.[1] For the accuracy level we are considering, the one-loop conversion relation is required

$$A_b^{\rm mixed} = A_b^{\overline{\rm DR}} + \Delta A_b\,, \quad \text{where} \quad \Delta A_b = \delta A_b^{\overline{\rm DR}} - \delta A_b^{\rm mixed}\,. \tag{5.1}$$

The counterterms δA_b^i were defined in eq. (3.6) and the superscript i indicates the renormalization scheme. The shift ΔA_b is a finite quantity as it can be explicitly checked. It depends in turn on the running bottom quark mass in the MSSM. We use an iterative method and choose the running bottom quark mass in the SM as the initial parameter. A stable solution is obtained after few iterations. In addition, the energy evolution of the parameter A_b has to be taken into account. We use here the one-loop RGE, that can be derived from eq. (3.6).

The dependence on the decoupling scale for $\alpha_s(\mu_{\rm GUT})$ is displayed in figure 2. The dotted, dashed and solid lines denote the one-, two-, and three-loop running, where the corresponding exact results for the decoupling coefficients have been implemented. One can see the improved stability of the three-loop results w.r.t. the decoupling-scale variation. The uncertainty induced by the current experimental accuracy on $\alpha_s(M_Z)$, $\delta\alpha_s = 0.001$ [26], is indicated by the hatched band.

In order to get an idea of the effects induced by the SUSY mass parameters on $\alpha_s(\mu_{\rm GUT})$, we show through the dash-dotted line the three-loop results if the SUSY parameters corresponding to the Snowmass Point SPS2 [55] are adopted. Their explicit values are: $m_{\tilde{g}} = 784.4\,\text{GeV}$, $m_{\tilde{t}_1} = 1003.9\,\text{GeV}$, $m_{\tilde{t}_2} = 1307.4\,\text{GeV}$, $m_{\tilde{b}_1} = 1296.6\,\text{GeV}$, $m_{\tilde{b}_2} = 1520.1\,\text{GeV}$, and $\tan\beta = 10.0$. The curves induced by the other benchmark points SPSi, with $i = 3, 4, \ldots, 9$ would lie between the two curves displayed here. One clearly notices the great impact of the SUSY-mass pattern on the predicted value of the strong coupling at high energies. Accordingly, for precision studies the explicit mass pattern of heavy particles must be taken into account.

[1] See ref. [54] for a detailed discussion.

JHEP02(2009)037

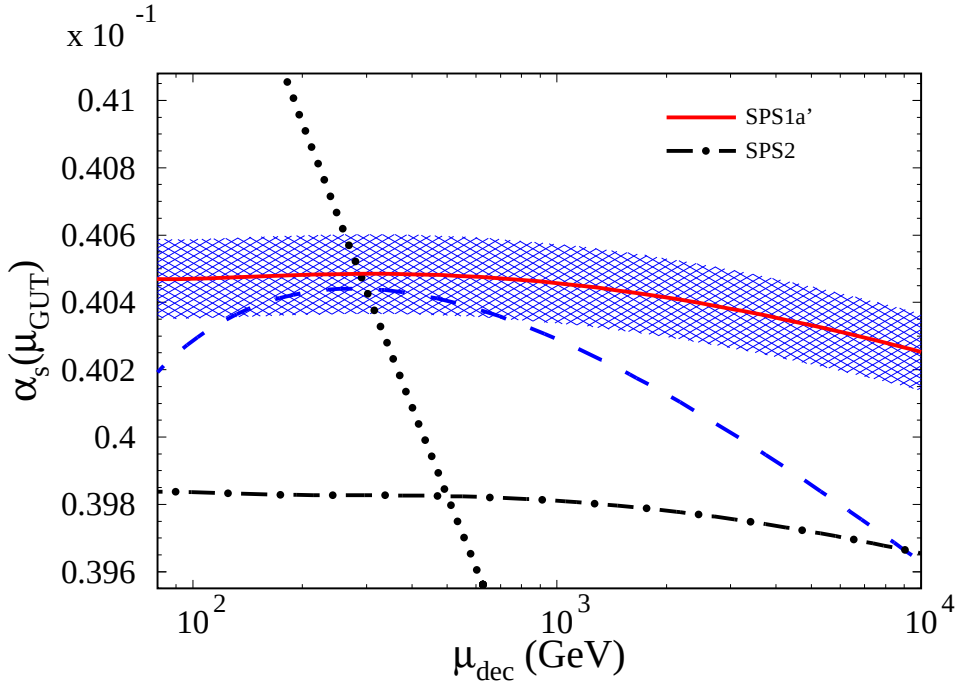

Figure 2: $\alpha_s(\mu_{\rm GUT})$ as a function of $\mu_{\rm dec}$. Dotted, dashed and solid lines denote the one-, two-, and three-loop contributions, respectively, obtained by using for the input parameters their values for the SPS1a′ benchmark point. The dash-dotted line shows the three-loop running corresponding to the SPS2 point.

In figure 3 the scale dependence for $m_b(\mu_{\rm GUT})$ is shown. The fine-dotted, dashed and solid lines correspond to the exact one-, two-, and three-loop running obtained in the SPS1a′ scenario. As explained above, the energy evolution of the running parameters have to be combined with the appropriate matching conditions between the low- and high-energy regimes. More explicitly, in case of m_b we determine its value within SQCD at the energy-scale $\mu_{\rm dec}$ through the relation

$$m_b^{\rm SQCD}(\mu_{\rm dec}) = \frac{m_b^{(5)}(\mu_{\rm dec})}{\zeta_{m_b}(\mu_{\rm dec})}\,, \quad \text{where} \quad \frac{1}{\zeta_{m_b}} = \frac{1}{1+\delta\zeta_{m_b}^{\tan\beta}+\delta\zeta_{m_b}^{\rm rest}}\,. \tag{5.2}$$

Here $\delta\zeta_{m_b}^{\tan\beta}$ denotes the contributions proportional with $\tan\beta$ and $\delta\zeta_{m_b}^{\rm rest}$ the remaining corrections. For simplicity, we do not show in eq. (5.2) the explicit dependence on the MSSM parameters. For the i-loop running analysis, we take into account the $(i-1)$-loop contribution to the eq. (5.2). As can be seen from the figure 3, the three-loop results stabilize the scale dependence and reduce further the theoretical uncertainty.

The dotted line displays the two-loop running bottom-mass, where the contributions proportional with $\tan\beta$ to the one-loop ζ_{m_b} are resummed following the method proposed

JHEP02(2009)037

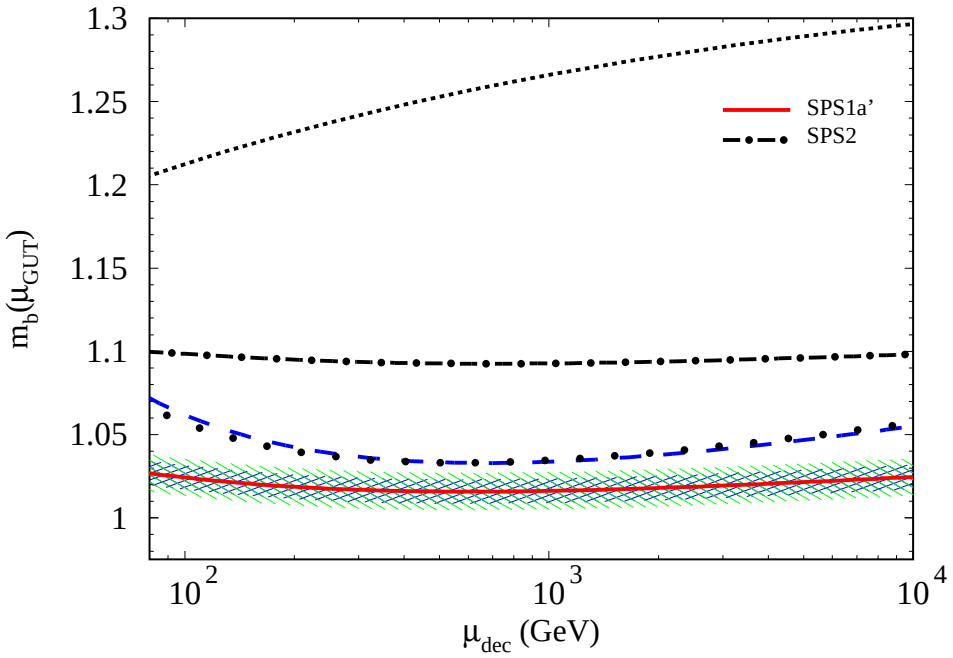

Figure 3: $m_b(\mu_{\rm GUT})$ as a function of $\mu_{\rm dec}$. The fine-dotted, dashed and solid lines denote the one-, two-, and three-loop contributions to the running bottom mass for SPS1a′ benchmark point, respectively. The dotted line displays the two-loop running, where the $\tan\beta$ enhanced contributions are resummed according to ref. [30]. The dash-dotted line represents the three-loop running corresponding to the SPS2 benchmark point.

in refs. [30, 13]. Within this approach, the matching condition can be written as

$$m_b^{\rm SQCD}(\mu_{\rm dec}) = \frac{m_b^{(5)}(\mu_{\rm dec})}{\zeta_{m_b}^{1-\rm loop}(\mu_{\rm dec})} \quad \text{and} \quad \frac{1}{\zeta_{m_b}^{1-\rm loop}} = \frac{1-\delta\zeta_{m_b}^{\rm rest,1-loop}}{1+\delta\zeta_{m_b}^{\tan\beta,1-\rm loop}}\,. \tag{5.3}$$

The superscript $1-$loop indicates the order in perturbation theory at which the individual contributions are evaluated. The authors of ref. [30] showed that, for a consistent analysis not only the $\tan\beta$-enhanced contributions have to be resummed, but also the next-to-leading logarithms (NLL) $\alpha_s^{i+1}\ln^i(\mu^2/m_b^2)$. In our approach based on i-loop RGEs and $(i-1)$-loop decoupling coefficients the NLL are implicitly resummed. The very good agreement between the two computations can be explained by the fact that at one-loop order $\delta\zeta_{m_b}^{\rm rest}$ is almost an order of magnitude smaller than $\delta\zeta_{m_b}^{\tan\beta}$.

The experimental uncertainty generated by $\delta\,\alpha_s = 0.001$ [26] corresponds to the wider hatched band, and the one due to $\delta\,m_b = 25\,\text{MeV}$ [27] to the narrow band. Let us notice that the three-loop order effects exceed the uncertainty due to current experimental accuracy $\delta\alpha_s$.

Finally, the dash-dotted line shows the three-loop running if the SPS2 scenario is implemented. The differences between the three-loop order results are mainly due to the change of masses of the SUSY particles.

JHEP02(2009)037

$\mu_{\rm ren} = 1000\,{\rm GeV}$					
$\alpha_s(\mu_{\rm ren})$	0.0929	$\pm 0.0006\vert_{\delta\,\alpha_s(M_Z)}$		$-0.003\vert_{\rm SPS2}$	$\pm 0.0001\vert_{\rm th}$
$m_b(\mu_{\rm ren})$	2.164	$\pm 0.017\vert_{\delta\,\alpha_s(M_Z)}$	$\pm 0.015\vert_{\delta\,m_b(m_b)}$	$+0.12\vert_{\rm SPS2}$	$\pm 0.01\vert_{\rm th}$

$\mu_{\rm ren} = \mu_{\rm GUT}$					
$\alpha_s(\mu_{\rm ren})$	0.0405	$\pm 0.0001\vert_{\delta\,\alpha_s(M_Z)}$		$\pm 0.0007\vert_{\rm SPS2}$	$\pm 0.0001\vert_{\rm th}$
$m_b(\mu_{\rm ren})$	1.016	$\pm 0.011\vert_{\delta\,\alpha_s(M_Z)}$	$\pm 0.007\vert_{\delta\,m_b(m_b)}$	$+0.077\vert_{\rm SPS2}$	$\pm 0.005\vert_{\rm th}$

Table 1: Numerical results for the strong coupling and bottom-quark mass for $\mu = 1000\,{\rm GeV}$ and $\mu = \mu_{\rm GUT}$, respectively. The experimental inaccuracy is evaluated taking into account the present uncertainty on $\alpha_s(M_Z)$ and $m_b(m_b)$. The effects of the SUSY-mass parameters are evaluated w.r.t. the SPS2 benchmark point. The theoretical uncertainties due to unknown higher order corrections are estimated from the variation with the decoupling scale for $100\,{\rm GeV} \leq \mu_{\rm dec} \leq 1\,{\rm TeV}$.

For quantitative comparison, we give in table 1 the numerical values for $\alpha_s(\mu_{\rm ren})$ and $m_b(\mu)$ for $\mu_{\rm ren} = 1000\,{\rm GeV}$ and $\mu_{\rm ren} = \mu_{\rm GUT}$, evaluated with three-loop accuracy. For the decoupling scale we choose $\mu_{\rm dec} = 600\,{\rm GeV}$ as at this scale the difference between the two- and three-loop order corrections reaches a minimum. The different sources of uncertainties are explicitly displayed. The theoretical uncertainties due to unknown higher order corrections are estimated from the variation of the three-loop results when the decoupling scale is modified from 100 GeV to 1 TeV. The effects of the SUSY-mass parameters are evaluated as the difference between the three-loop results corresponding to the benchmark points SPS1a′ and SPS2. One can easily see that the impact of the SUSY-mass pattern is at least five times larger than the experimental accuracy.

As already pointed out in the previous sections the unification of the Yukawa couplings is very sensitive to the MSSM parameters. The dependence on the soft SUSY breaking parameters is induced in our approximation only through the decoupling coefficients. They comprise an explicit dependence through the X_b parameter (in the case of ζ_{m_b}) and an implicit one through the squark masses.

The analytical formulae for ζ_s and ζ_m given in section 4.2 are expressed in terms of the physical squark masses. Since they are not known experimentally, for the following numerical analyses, we computed them making the assumption that the soft SUSY breaking mass parameters defined in the on-shell scheme obey the following relation $M_{\tilde{Q}}(t) = M_{\tilde{D}}(\tilde{M}) = M_{\tilde{U}}(\tilde{M}) = A_f = \pm\mu = \tilde{M}$, where $M_{\tilde{Q}}(t)$ is the on-shell input parameter in the stop-mass matrix.[2] The corresponding input parameter in the sbottom-mass matrix acquires a finite shift of $\mathcal{O}(\alpha_s)$ [56]. Upon diagonalization of the squark-mass matrices eq. (3.1), one obtains the on-shell squark masses $m_{\tilde{q}_{1,2}}$. The parameter A_b entering through X_b the one-loop results have to be converted from the on-shell scheme in the renormalization scheme we introduced in section 2.

In order to estimate the phenomenological impact, we discuss the difference between

[2]See section 3 for definitions and refs. [56, 57] for a comprehensive discussion.

JHEP02(2009)037

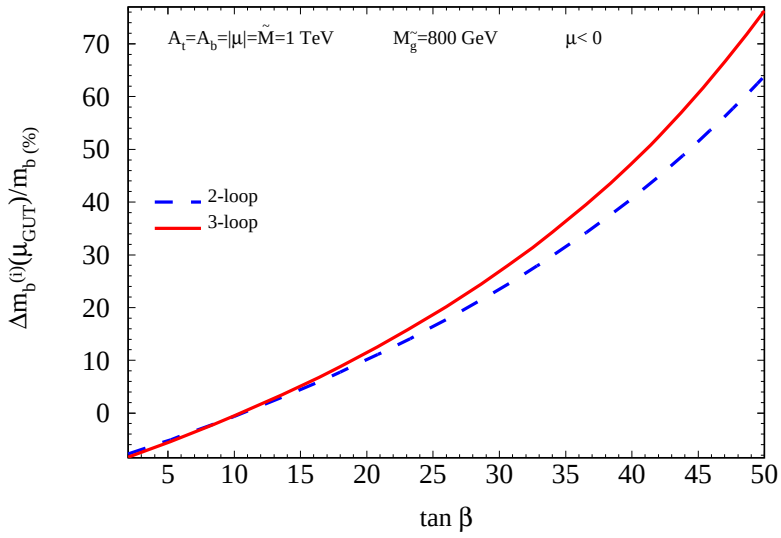

(a)

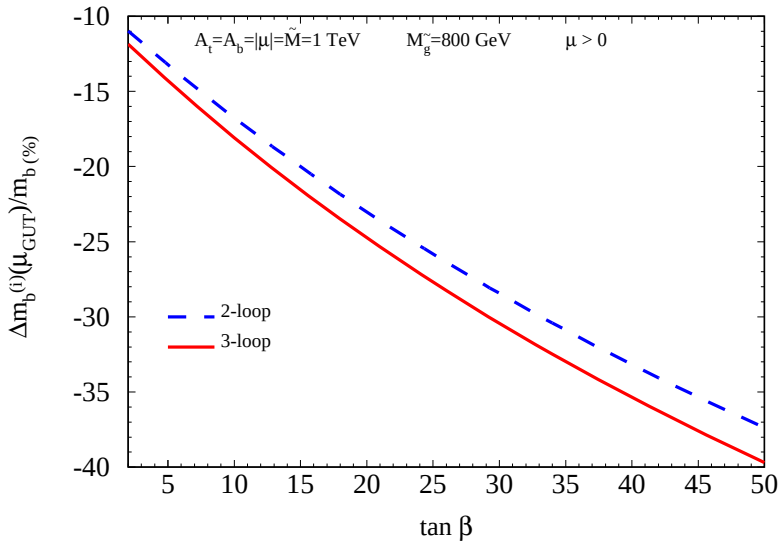

(b)

Figure 4: $\Delta m_b/m_b$ as a function of $\tan\beta$ for $\mu < 0$ (a) and $\mu > 0$ (b). The soft SUSY breaking mass parameters are fixed to 1 TeV and the gluino mass to $M_{\tilde{g}} = 800\,\text{GeV}$.

$m_b(\mu_{\text{GUT}})$ evaluated using i-loop running and $(i-1)$-loop decoupling and the one-loop result

$$\frac{\Delta m_b^{(\text{i})}}{m_b} = \frac{m_b^{(\text{i-loop})} - m_b^{(\text{1-loop})}}{m_b^{(\text{1-loop})}}\,. \tag{5.4}$$

JHEP02(2009)037

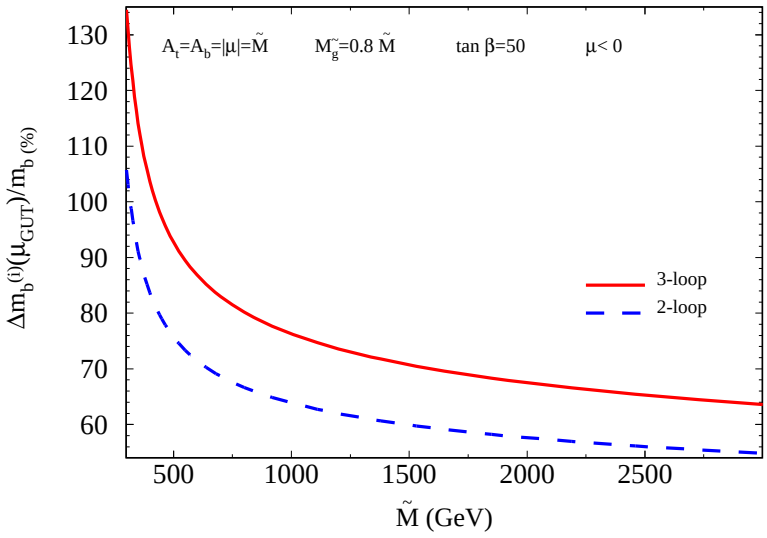

(a)

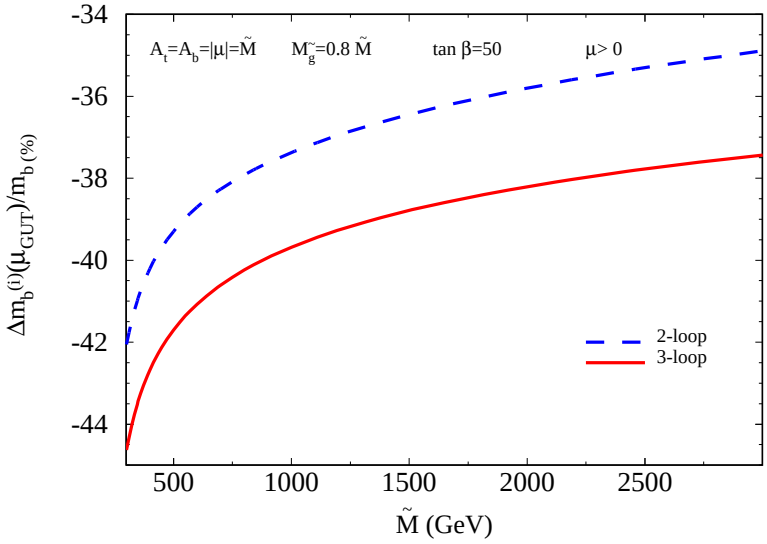

(b)

Figure 5: $\Delta m_b/m_b$ as a function of $\tilde{M}$ for $\mu < 0$ (a) and $\mu > 0$ (b). $\tan\beta$ is fixed to 50 and the gluino mass is $M_{\tilde{g}} = 0.8\tilde{M}$.

In figure 4 we fix the soft SUSY breaking mass parameters to $\tilde{M} = 1\,\text{TeV}$ and $M_{\tilde{g}} = 800\,\text{GeV}$, and study the dependence of $\Delta\, m_b^{(\text{i})}$ for $i = 2$ (dashed) and $i = 3$ (solid line) as a function of $\tan\beta$. One can clearly see the abrupt increase/decrease of the two- and three-loop order radiative corrections with the increase of $\tan\beta$. Whereas the effects of the

JHEP02(2009)037

the one-loop decoupling can be as large as 65% for $\mu_{\rm SUSY} < 0$ and -37% for $\mu_{\rm SUSY} > 0$, the two-loop corrections are moderate, reaching at most 10% and -3%, respectively.

The numerical effects for large values of $\tan\beta$ are of special interest for the study of Yukawa-coupling unification. In figure 5 we show $\Delta\, m_b^{(\rm i)}$ as a function of the soft SUSY breaking mass scale for $\tan\beta = 50$. One can see the increase in size of radiative corrections for lighter SUSY masses. Again, for $\mu_{\rm SUSY} > 0$ the bulk of the corrections are comprised in the two-loop running mass, while the three-loop order effects sum up to few percent. For $\mu_{\rm SUSY} < 0$ and light SUSY masses the three-loop contributions can increase the bottom-quark mass with up to 30%.

6. Conclusions

The knowledge of fundamental parameters at high energies, such as $\tilde{M}$ or $\mu_{\rm GUT}$, are essential for the reconstruction of the theory beyond the SM. In this paper we presented the exact two-loop decoupling coefficients of the strong coupling and the bottom-quark mass within the SQCD. Together with the known three-loop order RGEs they allow predictions of the two parameters at high energies with three-loop accuracy. This level of precision on the theory side is necessary in order to match with the current experimental accuracy. The values of the gauge and Yukawa couplings at the unification scale $\mu_{\rm GUT}$ are essential ingredients for the determination of the GUT threshold corrections, which in turn are used to identify the underlying GUT model.
In addition, the dependence on the energy scale at which the supersymmetric particles are integrated out, which reflects the size of the unknown higher order corrections, is significantly reduced in the case of the three-loop order predictions.

Furthermore, the approach outlined here accounts for the effects induced by the individual mass parameters. They are phenomenologically significant for both parameters and exceed the experimental uncertainty by more than a factor five.

The radiative corrections to the running bottom-quark mass are particularly important for SUSY models with large values of $\tan\beta$. It turns out that for negative values of $\mu_{\rm SUSY}$ the three-loop order contributions can reach up to 30% from the tree-level bottom-quark mass. Furthermore, they clearly stabilize the perturbative behaviour. These features render them indispensable for studies concerning the Yukawa-coupling unification.

Acknowledgments

We would like to thank M. Steinhauser for his continuous support and numerous inspiring discussions and suggestions. We also thank him and R. Harlander for carefully reading the manuscript. L.M. is grateful to K.G. Chetyrkin for enlightening conversations concerning the decoupling approach.

We thank A. V. Bednyakov for providing us with the results necessary for the numerical comparison with Ref [39].

This work was supported by the DFG through SFB/TR 9 and by the Graduiertenkolleg "Hochenergiephysik und Teilchenastrophysik".

References

[1] S. Dimopoulos, S. Raby and F. Wilczek, *Supersymmetry and the scale of unification*, *Phys. Rev.* **D 24** (1981) 1681.

[2] L.E. Ibáñez and G.G. Ross, *Low-energy predictions in supersymmetric grand unified theories*, *Phys. Lett.* **B 105** (1981) 439.

[3] U. Amaldi, W. de Boer and H. Furstenau, *Comparison of grand unified theories with electroweak and strong coupling constants measured at LEP*, *Phys. Lett.* **B 260** (1991) 447.

[4] H. Georgi and S.L. Glashow, *Unity of all elementary particle forces*, *Phys. Rev. Lett.* **32** (1974) 438.

[5] H. Fritzsch and P. Minkowski, *Unified interactions of leptons and hadrons*, *Ann. Phys. (NY)* **93** (1975) 193.

[6] P. Langacker and N. Polonsky, *Implications of Yukawa unification for the Higgs sector in supersymmetric grand unified models*, *Phys. Rev.* **D 50** (1994) 2199 [hep-ph/9403306].

[7] L.J. Hall, R. Rattazzi and U. Sarid, *The top quark mass in supersymmetric $SO(10)$ unification*, *Phys. Rev.* **D 50** (1994) 7048 [hep-ph/9306309].

[8] J.L. Diaz-Cruz, H. Murayama and A. Pierce, *Can supersymmetric loops correct the fermion mass relations in $SU(5)$?*, *Phys. Rev.* **D 65** (2002) 075011 [hep-ph/0012275].

[9] R. Hempfling, *Yukawa coupling unification with supersymmetric threshold corrections*, *Phys. Rev.* **D 49** (1994) 6168.

[10] M.S. Carena, M. Olechowski, S. Pokorski and C.E.M. Wagner, *Electroweak symmetry breaking and bottom - top Yukawa unification*, *Nucl. Phys.* **B 426** (1994) 269 [hep-ph/9402253].

[11] K. Tobe and J.D. Wells, *Revisiting top-bottom-τ Yukawa unification in supersymmetric grand unified theories*, *Nucl. Phys.* **B 663** (2003) 123 [hep-ph/0301015].

[12] G.A. Blair, W. Porod and P.M. Zerwas, *The reconstruction of supersymmetric theories at high energy scales*, *Eur. Phys. J.* **C 27** (2003) 263 [hep-ph/0210058].

[13] J.A. Aguilar-Saavedra et al., *Supersymmetry parameter analysis: spa convention and project*, *Eur. Phys. J.* **C 46** (2006) 43 [hep-ph/0511344].

[14] F.E. Paige, S.D. Protopopescu, H. Baer and X. Tata, *ISAJET* 7.69*: a Monte Carlo event generator for pp, $\bar{p}p$ and e^+e^- reactions*, hep-ph/0312045.

[15] B.C. Allanach, *SOFTSUSY: a C++ program for calculating supersymmetric spectra*, *Comput. Phys. Commun.* **143** (2002) 305 [hep-ph/0104145].

[16] W. Porod, *SPheno, a program for calculating supersymmetric spectra, SUSY particle decays and SUSY particle production at e^+e^- colliders*, *Comput. Phys. Commun.* **153** (2003) 275 [hep-ph/0301101].

[17] A. Djouadi, J.-L. Kneur and G. Moultaka, *SuSpect: a Fortran code for the supersymmetric and Higgs particle spectrum in the MSSM*, *Comput. Phys. Commun.* **176** (2007) 426 [hep-ph/0211331].

[18] S.P. Martin and M.T. Vaughn, *Regularization dependence of running couplings in softly broken supersymmetry*, *Phys. Lett.* **B 318** (1993) 331 [hep-ph/9308222].

JHEP02(2009)037

[19] S.P. Martin and M.T. Vaughn, *Two loop renormalization group equations for soft supersymmetry breaking couplings*, *Phys. Rev.* **D 50** (1994) 2282 [*Erratum ibid.* **D 78** (2008) 039903] [hep-ph/9311340].

[20] I. Jack and D.R.T. Jones, *Soft supersymmetry breaking and finiteness*, *Phys. Lett.* **B 333** (1994) 372 [hep-ph/9405233].

[21] Y. Yamada, *Two loop renormalization group equations for soft SUSY breaking scalar interactions: supergraph method*, *Phys. Rev.* **D 50** (1994) 3537 [hep-ph/9401241].

[22] D.M. Pierce, J.A. Bagger, K.T. Matchev and R.-J. Zhang, *Precision corrections in the minimal supersymmetric standard model*, *Nucl. Phys.* **B 491** (1997) 3 [hep-ph/9606211].

[23] B.C. Allanach, S. Kraml and W. Porod, *Theoretical uncertainties in sparticle mass predictions from computational tools*, *JHEP* **03** (2003) 016 [hep-ph/0302102].

[24] R. Harlander, L. Mihaila and M. Steinhauser, *Two-loop matching coefficients for the strong coupling in the MSSM*, *Phys. Rev.* **D 72** (2005) 095009 [hep-ph/0509048].

[25] R.V. Harlander, L. Mihaila and M. Steinhauser, *Running of α_s and m_b in the MSSM*, *Phys. Rev.* **D 76** (2007) 055002 [arXiv:0706.2953].

[26] S. Bethke, *Experimental tests of asymptotic freedom*, *Prog. Part. Nucl. Phys.* **58** (2007) 351 [hep-ex/0606035].

[27] J.H. Kühn, M. Steinhauser and C. Sturm, *Heavy quark masses from sum rules in four-loop approximation*, *Nucl. Phys.* **B 778** (2007) 192 [hep-ph/0702103].

[28] D. Noth and M. Spira, *Higgs boson couplings to bottom quarks: two-loop supersymmetry-QCD corrections*, *Phys. Rev. Lett.* **101** (2008) 181801 [arXiv:0808.0087].

[29] T. Blazek, R. Dermisek and S. Raby, *Yukawa unification in $SO(10)$*, *Phys. Rev.* **D 65** (2002) 115004 [hep-ph/0201081].

[30] M.S. Carena, D. Garcia, U. Nierste and C.E.M. Wagner, *Effective Lagrangian for the $\bar{t}bH^+$ interaction in the MSSM and charged Higgs phenomenology*, *Nucl. Phys.* **B 577** (2000) 88 [hep-ph/9912516].

[31] W.A. Bardeen, A.J. Buras, D.W. Duke and T. Muta, *Deep inelastic scattering beyond the leading order in asymptotically free gauge theories*, *Phys. Rev.* **D 18** (1978) 3998.

[32] W. Siegel, *Supersymmetric dimensional regularization via dimensional reduction*, *Phys. Lett.* **B 84** (1979) 193.

[33] T. Appelquist and J. Carazzone, *Infrared singularities and massive fields*, *Phys. Rev.* **D 11** (1975) 2856.

[34] K.G. Chetyrkin, B.A. Kniehl and M. Steinhauser, *Decoupling relations to $O(\alpha_s^3)$ and their connection to low-energy theorems*, *Nucl. Phys.* **B 510** (1998) 61 [hep-ph/9708255].

[35] M. Steinhauser, *Results and techniques of multi-loop calculations*, *Phys. Rept.* **364** (2002) 247 [hep-ph/0201075].

[36] P.M. Ferreira, I. Jack and D.R.T. Jones, *The three-loop SSM β-functions*, *Phys. Lett.* **B 387** (1996) 80 [hep-ph/9605440].

[37] Y. Schroder and M. Steinhauser, *Four-loop decoupling relations for the strong coupling*, *JHEP* **01** (2006) 051 [hep-ph/0512058].

JHEP02(2009)037

[38] K.G. Chetyrkin, J.H. Kuhn and C. Sturm, *QCD decoupling at four loops*, *Nucl. Phys.* **B 744** (2006) 121 [hep-ph/0512060].

[39] A.V. Bednyakov, *Running mass of the b-quark in QCD and SUSY QCD*, *Int. J. Mod. Phys.* **A 22** (2007) 5245 [arXiv:0707.0650].

[40] A. Bednyakov, A. Onishchenko, V. Velizhanin and O. Veretin, *Two-loop $O(\alpha_s^2)$ MSSM corrections to the pole masses of heavy quarks*, *Eur. Phys. J.* **C 29** (2003) 87 [hep-ph/0210258].

[41] A.I. Davydychev and J.B. Tausk, *Two loop selfenergy diagrams with different masses and the momentum expansion*, *Nucl. Phys.* **B 397** (1993) 123.

[42] K.G. Chetyrkin and F.V. Tkachov, *Integration by parts: the algorithm to calculate β-functions in 4 loops*, *Nucl. Phys.* **B 192** (1981) 159.

[43] P. Nogueira, *Automatic Feynman graph generation*, *J. Comput. Phys.* **105** (1993) 279.

[44] T. Seidensticker, *Automatic application of successive asymptotic expansions of Feynman diagrams*, hep-ph/9905298.

[45] J.A.M. Vermaseren, *New features of FORM*, math-ph/0010025.

[46] J. Guasch, J. Solà and W. Hollik, *Yukawa-coupling corrections to scalar quark decays*, *Phys. Lett.* **B 437** (1998) 88 [hep-ph/9802329].

[47] I. Jack, D.R.T. Jones and K.L. Roberts, *Dimensional reduction in nonsupersymmetric theories*, *Z. Physik* **C 62** (1994) 161 [hep-ph/9310301].

[48] I. Jack, D.R.T. Jones, S.P. Martin, M.T. Vaughn and Y. Yamada, *Decoupling of the epsilon scalar mass in softly broken supersymmetry*, *Phys. Rev.* **D 50** (1994) 5481 [hep-ph/9407291].

[49] R. Harlander, P. Kant, L. Mihaila and M. Steinhauser, *Dimensional reduction applied to QCD at three loops*, *JHEP* **09** (2006) 053 [hep-ph/0607240].

[50] J.R. Ellis, M.K. Gaillard and D.V. Nanopoulos, *A phenomenological profile of the Higgs boson*, *Nucl. Phys.* **B 106** (1976) 292;
M.A. Shifman, A.I. Vainshtein and V.I. Zakharov, *Remarks on Higgs boson interactions with nucleons*, *Phys. Lett.* **B 78** (1978) 443;
M.A. Shifman, A.I. Vainshtein, M.B. Voloshin and V.I. Zakharov, *Low-energy theorems for Higgs boson couplings to photons*, *Sov. J. Nucl. Phys.* **30** (1979) 711 [*Yad. Fiz.* **30** (1979) 1368];
A.I. Vainshtein, V.I. Zakharov and M.A. Shifman, *Higgs particles*, *Sov. Phys. Usp.* **23** (1980) 429 [*Usp. Fiz. Nauk.* **131** (1980) 537];
B.A. Kniehl and M. Spira, *Low-energy theorems in Higgs physics*, *Z. Physik* **C 69** (1995) 77 [hep-ph/9505225];
W. Kilian, *Renormalized soft Higgs theorems*, *Z. Physik* **C 69** (1995) 89 [hep-ph/9505309];
M. Spira, A. Djouadi, D. Graudenz and P.M. Zerwas, *Higgs boson production at the LHC*, *Nucl. Phys.* **B 453** (1995) 17 [hep-ph/9504378].

[51] J. Guasch, P. Hafliger and M. Spira, *MSSM Higgs decays to bottom quark pairs revisited*, *Phys. Rev.* **D 68** (2003) 115001 [hep-ph/0305101].

[52] Particle Data Group collaboration, W.M. Yao et al., *Review of particle physics*, *J. Phys.* **G 33** (2006) 1.

JHEP02(2009)037

[53] Tevatron Electroweak Working Group collaboration and others, *Combination of CDF and D0 results on the mass of the top quark*, arXiv:0808.1089.

[54] S. Heinemeyer, W. Hollik, H. Rzehak and G. Weiglein, *High-precision predictions for the MSSM Higgs sector at $O(\alpha_b\alpha_s)$*, *Eur. Phys. J.* **C 39** (2005) 465 [hep-ph/0411114].

[55] N. Ghodbane and H.-U. Martyn, *Compilation of SUSY particle spectra from Snowmass* 2001 *benchmark models*, in *Proceedings of the APS/DPF/DPB Summer Study on the Future of Particle Physics (Snowmass* 2001, N. Graf ed., U.S.A. (2001) [hep-ph/0201233].

[56] A. Bartl et al., *QCD corrections to Higgs boson decays into squarks in the minimal supersymmetric standard model*, *Phys. Lett.* **B 402** (1997) 303 [hep-ph/9701398].

[57] A. Djouadi et al., *Leading QCD corrections to scalar quark contributions to electroweak precision observables*, *Phys. Rev.* **D 57** (1998) 4179 [hep-ph/9710438].

JHEP02(2009)037